

A FAST ALGORITHM FOR THE ELECTROMAGNETIC SCATTERING FROM A LARGE RECTANGULAR CAVITY IN THREE DIMENSIONS

YANLI CHEN, XUE JIANG, JUN LAI, AND PEIJUN LI

ABSTRACT. The paper is concerned with the three-dimensional electromagnetic scattering from a large open rectangular cavity that is embedded in a perfectly electrically conducting infinite ground plane. By introducing a transparent boundary condition, the scattering problem is formulated into a boundary value problem in the bounded cavity. Based on the Fourier expansions of the electric field, the Maxwell equation is reduced to one-dimensional ordinary differential equations for the Fourier coefficients. A fast algorithm, employing the fast Fourier transform and the Gaussian elimination, is developed to solve the resulting linear system for the cavity which is filled with either a homogeneous or a layered medium. In addition, a novel scheme is designed to evaluate rapidly and accurately the Fourier transform of singular integrals. Numerical experiments are presented for large cavities to demonstrate the superior performance of the proposed method.

1. INTRODUCTION

The electromagnetic scattering from large cavities has received much attention in both engineering and mathematical communities due to its significant industrial and military applications [3, 6, 8, 10, 13]. For instance, the radar cross section (RCS) measures the detectability of a target by a radar system. In practice, the cavity RCS caused by objects such as jet engine inlet ducts, exhaust nozzles and cavity-backed antennas can dominate the total RCS. Therefore, mathematical and computational methods to accurately predict the cavity RCS are important for the enhancement or reduction of the total RCS [4, 5]. Another example is the non-destructive testing to determine the shape of a cavity embedded in a known object. In these applications, it has played a crucial role to have an efficient forward solver for the optimal design problems of reducing or enhancing the cavity RCS and the inverse problems of determining an unknown cavity.

A variety of numerical methods, including finite difference methods, finite element methods, the moment methods, boundary element methods, and hybrid methods, have been developed to solve the open cavity problems [9, 11, 16, 19–22, 24]. In particular, Bao and Sun [6] proposed a finite difference based fast algorithm for the two-dimensional electromagnetic scattering from large cavities. In the algorithm, an FFT-sine transform in the horizontal direction and the Gaussian elimination along the vertical direction were used to reduce the global system to a much smaller system imposed only on the open aperture of the cavity. As an extension of this method, a tensor product finite element method was proposed in [8] by employing piecewise polynomials of degree $k \geq 1$ to approximate the solution space of the cavity problem. In [26], a fourth order finite difference scheme was developed to discretize the cavity scattering problem in the rectangular domain and to reach a global fourth order convergence in the whole computational domain by a special treatment on the boundary condition. Since the resulting linear system obtained from the cavity problem is usually indefinite and ill-conditioned, convergence of iterative methods such as GMRES is very slow. Different kinds of preconditioners were proposed to accelerate the convergence [6–8, 26, 27]. On the other hand, a fast direct solver based on hierarchical matrix factorization technique was used to solve the two-dimensional electromagnetic scattering from an arbitrarily shaped cavity [13]. It was shown that the linear system resulted from the integral equation method can be solved in nearly linear time. The method was extended to the scattering of three-dimensional axis-symmetric cavities in [14]. We

2010 *Mathematics Subject Classification.* 78A40, 78M25.

Key words and phrases. electromagnetic scattering problem, Maxwell's equations, open cavity, fast algorithm.

refer to [12] for the motivation, modeling, computation, as well as related references on the open cavity scattering problems.

It is worth mentioning that the computation is extremely challenging when the cavities are large compared to the wavelength of the incident wave because of the highly oscillatory nature of the fields. For such a high frequency scattering problem, it is shown that the ratio of the error by the usual Galerkin type method and the error of the best approximation tends to infinity as the wave number increases [1, 2]. Due to these difficulties, the discretization by conventional numerical methods becomes very expensive for the large cavity scattering problems especially in three dimensions. In this paper, we intend to develop a fast algorithm for solving the three-dimensional electromagnetic scattering from large rectangular cavities embedded in an infinite perfectly electrically conducting ground plane.

More specifically, we consider the three-dimensional Maxwell equations along with the Silver–Müller radiation condition imposed at infinity. By using the dyadic Green’s function in the half space, we first derive an exact transparent boundary condition (TBC) on the open aperture of the cavity. As a result, the original scattering problem is formulated equivalently to a boundary value problem of Maxwell equations in a bounded domain. Secondly, we introduce the Fourier series expansion of the electric field inside the cavity. By such an expansion, the governing Maxwell equations can be reduced to one-dimensional ordinary differential equations with respect to the vertical direction. A second-order finite difference scheme is adopted to solve the ordinary differential systems. A fast algorithm, based on the fast Fourier transform in the horizontal directions and the Gaussian elimination along the vertical direction, is developed to solve the linear system arising from scattering of large cavities which may be filled with a homogeneous medium or a vertically layered medium. Moreover, we reduce the global system to a linear system on the open aperture of the cavity only and design a novel scheme to evaluate rapidly and accurately the singular integrals appeared in the transparent boundary condition. Numerical results show that our algorithm is very efficient in terms of computational cost.

The paper is organized as follows. In Section 2, we describe the problem formulation of the electromagnetic scattering by a rectangular cavity which is filled with a homogeneous medium. The governing Maxwell equations along with the Silver–Müller radiation condition are introduced. The TBC is presented to reduce the unbounded scattering problem to a boundary value problem formulated in the bounded cavity. The details of the fast algorithm are given in Section 3. Section 4 is devoted to an extension of the fast algorithm to the scattering of a cavity which is filled with a layered medium. Section 5 proposes an FFT based efficient algorithm to evaluate the singular integrals arising from the nonlocal TBC on the open aperture of the cavity. Analysis on the computational complexity for the fast algorithm is discussed in Section 6. Numerical examples are presented in Section 7 to demonstrate the performance of the proposed algorithm. The paper is concluded with some general remarks in Section 8.

2. PROBLEM FORMULATION

Consider the incidence of a time-harmonic electromagnetic wave on a rectangular cavity $D \subset \mathbb{R}^3$, which is embedded in the infinite ground plane Γ_g . The problem geometry is shown in Figure 1. The cavity wall S and the ground plane Γ_g are assumed to be perfect electric conductors. We also assume that the open aperture $\Gamma = [0, a] \times [0, b]$ is aligned with the ground plane Γ_g and the depth of the cavity is c . The half space above the ground and the cavity are assumed to be filled with some homogeneous material with a constant electric permittivity ε_0 and a constant magnetic permeability μ_0 . Let B_R^+ be a half-ball above the ground plane with hemisphere Γ_R^+ as part of the boundary, where the radius R is large enough so that Γ_R^+ covers the open aperture Γ . It is clear to note that the full boundary of ∂B_R^+ consists of the hemisphere Γ_R^+ , the open aperture Γ , and a part of the ground plane Γ_g . Without confusion, we simply denote $\partial B_R^+ = \Gamma_R^+ \cup \Gamma \cup \Gamma_g$.

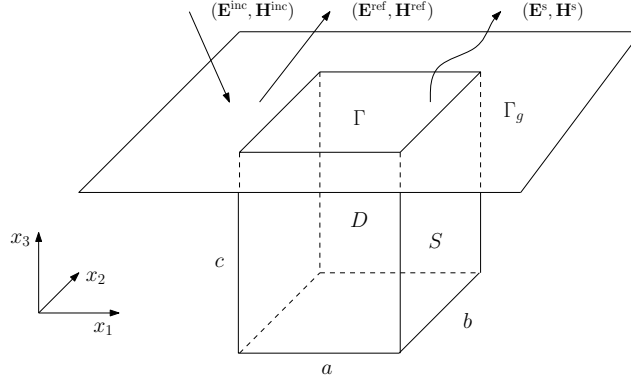


FIGURE 1. The problem geometry of the electromagnetic scattering by a rectangular cavity.

The total electric and magnetic fields (\mathbf{E}, \mathbf{H}) consist of the incident waves $(\mathbf{E}^{\text{inc}}, \mathbf{H}^{\text{inc}})$, the reflected waves $(\mathbf{E}^{\text{ref}}, \mathbf{H}^{\text{ref}})$ due to the infinite ground plane, and the scattered wave $(\mathbf{E}^{\text{s}}, \mathbf{H}^{\text{s}})$ because of the open cavity. The total fields \mathbf{E} and \mathbf{H} satisfy Maxwell's equations in $\mathbb{R}_+^3 \cup D$:

$$\nabla \times \mathbf{E} = i\omega\mu_0\mathbf{H}, \quad \nabla \times \mathbf{H} = -i\omega\varepsilon_0\mathbf{E}, \quad (2.1)$$

where $\omega > 0$ is the angular frequency. Since the ground plane and the cavity wall are perfect conductors, we have

$$\nu \times \mathbf{E} = 0 \quad \text{on } \Gamma_g \cup S, \quad (2.2)$$

where ν is the unit normal vector on Γ_g and S .

The incident electromagnetic plane waves $(\mathbf{E}^{\text{inc}}, \mathbf{H}^{\text{inc}})$ are given as

$$\mathbf{E}^{\text{inc}} = \mathbf{p}e^{i\mathbf{q}\cdot\mathbf{x}}, \quad \mathbf{H}^{\text{inc}} = \mathbf{s}e^{i\mathbf{q}\cdot\mathbf{x}}, \quad \mathbf{s} = \frac{\mathbf{q} \times \mathbf{p}}{\omega\mu_0}, \quad \mathbf{p} \cdot \mathbf{q} = 0,$$

where $\mathbf{x} = (x_1, x_2, x_3) \in \mathbb{R}^3$, $\mathbf{p} = (p_1, p_2, p_3)$ and $\mathbf{s} = (s_1, s_2, s_3)$ are the polarization vectors, $\mathbf{q} = (\alpha_1, \alpha_2, -\beta)$ with $\beta \geq 0$ is the propagation direction vector. It is easy to verify that the incident electromagnetic fields $(\mathbf{E}^{\text{inc}}, \mathbf{H}^{\text{inc}})$ satisfy the Maxwell equation (2.1) in \mathbb{R}_+^3 .

Due to the infinite ground plane, the reflected fields $(\mathbf{E}^{\text{ref}}, \mathbf{H}^{\text{ref}})$ can be explicitly written as

$$\mathbf{E}^{\text{ref}} = \mathbf{p}^*e^{i\mathbf{q}^*\cdot\mathbf{x}}, \quad \mathbf{H}^{\text{ref}} = \mathbf{s}^*e^{i\mathbf{q}^*\cdot\mathbf{x}}, \quad \mathbf{s}^* = \frac{\mathbf{q}^* \times \mathbf{p}^*}{\omega\mu_0}, \quad \mathbf{p}^* \cdot \mathbf{q}^* = 0,$$

where $\mathbf{p}^* = (-p_1, -p_2, p_3)$ and $\mathbf{q}^* = (\alpha_1, \alpha_2, \beta)$. Evidently, the reflected fields $(\mathbf{E}^{\text{ref}}, \mathbf{H}^{\text{ref}})$ also satisfy the Maxwell equation (2.1) in \mathbb{R}_+^3 . In particular, the following homogeneous Dirichlet boundary condition is satisfied for the incident and reflected electric fields on the ground plane:

$$\nu \times (\mathbf{E}^{\text{inc}} + \mathbf{E}^{\text{ref}}) = 0 \quad \text{on } \Gamma_g.$$

It follows from (2.1) and the incident and reflected electromagnetic fields that the scattered electromagnetic fields $(\mathbf{E}^{\text{s}}, \mathbf{H}^{\text{s}})$ also satisfy the Maxwell equation

$$\nabla \times \mathbf{E}^{\text{s}} = i\omega\mu_0\mathbf{H}^{\text{s}}, \quad \nabla \times \mathbf{H}^{\text{s}} = -i\omega\varepsilon_0\mathbf{E}^{\text{s}}, \quad \mathbf{x} \in \mathbb{R}_+^3, \quad (2.3)$$

and the homogeneous Dirichlet boundary condition

$$\nu \times \mathbf{E}^{\text{s}} = 0 \quad \text{on } \Gamma_g. \quad (2.4)$$

In addition, the scattered field $(\mathbf{E}^{\text{s}}, \mathbf{H}^{\text{s}})$ are required to satisfy the Silver–Müller radiation condition:

$$\sqrt{\varepsilon_0}\mathbf{E}^{\text{s}} - \sqrt{\mu_0}\mathbf{H}^{\text{s}} \times \hat{\mathbf{x}} = o(|\mathbf{x}|^{-1}), \quad |\mathbf{x}| \rightarrow \infty, \quad (2.5)$$

where $\hat{\mathbf{x}} = \mathbf{x}/|\mathbf{x}|$. By eliminating the scattered magnetic field in (2.3), the scattered electric field satisfies

$$\nabla \times (\nabla \times \mathbf{E}^{\text{s}}) - \kappa_0^2 \mathbf{E}^{\text{s}} = 0 \quad \text{in } \mathbb{R}_+^3, \quad (2.6)$$

where $\kappa_0 = \omega\sqrt{\varepsilon_0\mu_0}$ is the wavenumber.

In order to derive a transparent boundary condition on the open aperture Γ , we introduce the half-space dyadic Green's function $\bar{\bar{G}}_e(\mathbf{x}, \mathbf{y})$, which is given by

$$\bar{\bar{G}}_e(\mathbf{x}, \mathbf{y}) = \bar{\bar{G}}_0(\mathbf{x}, \mathbf{y}) - \bar{\bar{G}}_0(\mathbf{x}, \mathbf{y}_i) + 2\hat{\mathbf{z}}\hat{\mathbf{z}}g(\mathbf{x}, \mathbf{y}_i), \quad (2.7)$$

where

$$\bar{\bar{G}}_0(\mathbf{x}, \mathbf{y}) = \left(\bar{\bar{I}} - \frac{1}{\kappa_0^2} \nabla_{\mathbf{x}} \nabla_{\mathbf{y}} \right) g(\mathbf{x}, \mathbf{y}), \quad (2.8)$$

is the free space dyadic Green's function, $\bar{\bar{I}} = \hat{\mathbf{x}}\hat{\mathbf{x}} + \hat{\mathbf{y}}\hat{\mathbf{y}} + \hat{\mathbf{z}}\hat{\mathbf{z}}$ is the 3×3 identity matrix, and

$$g(\mathbf{x}, \mathbf{y}) = \frac{e^{i\kappa_0|\mathbf{x}-\mathbf{y}|}}{4\pi|\mathbf{x}-\mathbf{y}|}, \quad (2.9)$$

is the free space Green's function for the three-dimensional Helmholtz equation. Here $\mathbf{y}_i = y_1\hat{\mathbf{x}} + y_2\hat{\mathbf{y}} - y_3\hat{\mathbf{z}}$ denotes the image point of $\mathbf{y} = y_1\hat{\mathbf{x}} + y_2\hat{\mathbf{y}} + y_3\hat{\mathbf{z}}$, and $\hat{\mathbf{x}}, \hat{\mathbf{y}}, \hat{\mathbf{z}}$ are the unit vectors in the x_1, x_2, x_3 axis, respectively.

The half-space dyadic Green's function satisfies the Maxwell equation

$$\nabla \times (\nabla \times \bar{\bar{G}}_e(\mathbf{x}, \mathbf{y})) - \kappa_0^2 \bar{\bar{G}}_e(\mathbf{x}, \mathbf{y}) = \bar{\bar{I}}\delta(\mathbf{x} - \mathbf{y}) \quad \text{in } \mathbb{R}_+^3, \quad (2.10)$$

and the Dirichlet boundary condition

$$\nu \times \bar{\bar{G}}_e(\mathbf{x}, \mathbf{y}) = 0 \quad \text{on } \Gamma_g \cup \Gamma, \quad (2.11)$$

where δ is the Dirac delta function. Furthermore, the half-space dyadic Green's function satisfies the Silver–Müller radiation condition.

Next, we present the transparent boundary condition. Multiplying both sides of (2.6) by the half-space dyadic Green's function and integrating over B_R^+ , we obtain

$$\int_{B_R^+} \left((\nabla_{\mathbf{x}} \times \nabla_{\mathbf{x}} \times \mathbf{E}^s(\mathbf{x})) \cdot \bar{\bar{G}}_e(\mathbf{x}, \mathbf{y}) - \kappa_0^2 \mathbf{E}^s(\mathbf{x}) \cdot \bar{\bar{G}}_e(\mathbf{x}, \mathbf{y}) \right) d\mathbf{x} = 0.$$

It follows from the second vector Green's theorem that

$$\begin{aligned} & \int_{B_R^+} \mathbf{E}^s(\mathbf{x}) \cdot \left(\nabla_{\mathbf{x}} \times \nabla_{\mathbf{x}} \times \bar{\bar{G}}_e(\mathbf{x}, \mathbf{y}) - \kappa_0^2 \bar{\bar{G}}_e(\mathbf{x}, \mathbf{y}) \right) d\mathbf{x} \\ &= - \int_{\Gamma_R^+ \cup \Gamma_g} \left((\nu \times \mathbf{E}^s(\mathbf{x})) \cdot (\nabla_{\mathbf{x}} \times \bar{\bar{G}}_e(\mathbf{x}, \mathbf{y})) - (\nu \times \bar{\bar{G}}_e(\mathbf{x}, \mathbf{y})) \cdot (\nabla_{\mathbf{x}} \times \mathbf{E}^s(\mathbf{x})) \right) ds_{\mathbf{x}}. \end{aligned} \quad (2.12)$$

Since the scattered field $\mathbf{E}^s(\mathbf{x})$ and the half-space dyadic Green's function satisfy the Silver–Müller radiation condition, we get

$$\int_{\Gamma_R^+} \left((\nu \times \mathbf{E}^s(\mathbf{x})) \cdot (\nabla_{\mathbf{x}} \times \bar{\bar{G}}_e(\mathbf{x}, \mathbf{y})) - (\nu \times \bar{\bar{G}}_e(\mathbf{x}, \mathbf{y})) \cdot (\nabla_{\mathbf{x}} \times \mathbf{E}^s(\mathbf{x})) \right) ds_{\mathbf{x}} = 0. \quad (2.13)$$

Combining (2.4) and (2.11) gives

$$\int_{\Gamma_g} \left((\nu \times \mathbf{E}^s(\mathbf{x})) \cdot (\nabla_{\mathbf{x}} \times \bar{\bar{G}}_e(\mathbf{x}, \mathbf{y})) - (\nu \times \bar{\bar{G}}_e(\mathbf{x}, \mathbf{y})) \cdot (\nabla_{\mathbf{x}} \times \mathbf{E}^s(\mathbf{x})) \right) ds_{\mathbf{x}} = 0 \quad (2.14)$$

and

$$\int_{\Gamma} (\nu \times \bar{\bar{G}}_e(\mathbf{x}, \mathbf{y})) \cdot (\nabla_{\mathbf{x}} \times \mathbf{E}^s(\mathbf{x})) ds_{\mathbf{x}} = 0. \quad (2.15)$$

Using (2.12)–(2.15) yields

$$\begin{aligned} & \int_{B_R^+} \mathbf{E}^s(\mathbf{x}) \cdot \left(\nabla_{\mathbf{x}} \times \nabla_{\mathbf{x}} \times \bar{\bar{G}}_e(\mathbf{x}, \mathbf{y}) - \kappa_0^2 \bar{\bar{G}}_e(\mathbf{x}, \mathbf{y}) \right) d\mathbf{x} \\ &= - \int_{\Gamma} (\nu \times \mathbf{E}^s(\mathbf{x})) \cdot (\nabla_{\mathbf{x}} \times \bar{\bar{G}}_e(\mathbf{x}, \mathbf{y})) ds_{\mathbf{x}}. \end{aligned} \quad (2.16)$$

Substituting (2.10) into (2.16) and switching variables \mathbf{x} and \mathbf{y} , we get

$$\mathbf{E}^s(\mathbf{x}) = - \int_{\Gamma} (\boldsymbol{\nu} \times \mathbf{E}^s(\mathbf{y})) \cdot (\nabla_{\mathbf{y}} \times \bar{\bar{G}}_e(\mathbf{x}, \mathbf{y})) ds_{\mathbf{y}}.$$

Noting $\boldsymbol{\nu} = -\hat{\mathbf{z}}$ gives

$$\mathbf{E}^s(\mathbf{x}) = \int_{\Gamma} (\hat{\mathbf{z}} \times \mathbf{E}^s(\mathbf{y})) \cdot (\nabla_{\mathbf{y}} \times \bar{\bar{G}}_e(\mathbf{x}, \mathbf{y})) ds_{\mathbf{y}}.$$

It follows from $\mathbf{E}^s = \mathbf{E} - \mathbf{E}^{\text{inc}} - \mathbf{E}^{\text{ref}}$ and $\hat{\mathbf{z}} \times (\mathbf{E}^{\text{inc}} + \mathbf{E}^{\text{ref}}) = 0$ on Γ that

$$\mathbf{E} = \mathbf{E}^{\text{inc}} + \mathbf{E}^{\text{ref}} + \int_{\Gamma} (\hat{\mathbf{z}} \times \mathbf{E}(\mathbf{y})) \cdot (\nabla_{\mathbf{y}} \times \bar{\bar{G}}_e(\mathbf{x}, \mathbf{y})) ds_{\mathbf{y}}. \quad (2.17)$$

Substituting (2.7) into (2.17), we obtain

$$\mathbf{E} = \mathbf{E}^{\text{inc}} + \mathbf{E}^{\text{ref}} + 2 \int_{\Gamma} (\hat{\mathbf{z}} \times \mathbf{E}(\mathbf{y})) \cdot (\nabla_{\mathbf{y}} \times \bar{\bar{G}}_0(\mathbf{x}, \mathbf{y})) ds_{\mathbf{y}}. \quad (2.18)$$

Taking curl on the both sides of (2.18) yields

$$\nabla_{\mathbf{x}} \times \mathbf{E} = \nabla_{\mathbf{x}} \times \mathbf{E}^{\text{inc}} + \nabla_{\mathbf{x}} \times \mathbf{E}^{\text{ref}} - 2\kappa_0^2 \int_{\Gamma} (\hat{\mathbf{z}} \times \mathbf{E}(\mathbf{y})) \cdot \bar{\bar{G}}_0(\mathbf{x}, \mathbf{y}) ds_{\mathbf{y}}. \quad (2.19)$$

Substituting (2.8) into (2.19), we get

$$\begin{aligned} (\nabla_{\mathbf{x}} \times \mathbf{E}) &= \nabla_{\mathbf{x}} \times \mathbf{E}^{\text{inc}} + \nabla_{\mathbf{x}} \times \mathbf{E}^{\text{ref}} - 2\kappa_0^2 \int_{\Gamma} (\hat{\mathbf{z}} \times \mathbf{E}(\mathbf{y})) g(\mathbf{x}, \mathbf{y}) ds_{\mathbf{y}} \\ &\quad + 2 \left(\nabla_{\mathbf{x}} \int_{\Gamma} (\hat{\mathbf{z}} \times \mathbf{E}(\mathbf{y})) \cdot (\nabla_{\mathbf{y}} g(\mathbf{x}, \mathbf{y})) ds_{\mathbf{y}} \right). \end{aligned}$$

For a continuous differential function u defined in a neighborhood of Γ , define the surface gradient on Γ by

$$\nabla_{\Gamma} u = (\boldsymbol{\nu} \times \nabla u) \times \boldsymbol{\nu}.$$

Moreover, we have the decomposition

$$\nabla u = \nabla_{\Gamma} u + \frac{\partial u}{\partial \boldsymbol{\nu}} \boldsymbol{\nu}, \quad (2.20)$$

where $\frac{\partial u}{\partial \boldsymbol{\nu}}$ is the normal derivative on Γ . Let \mathbf{v} be a tangent vector on Γ , then we have

$$\int_{\Gamma} u \operatorname{div}_{\Gamma} \mathbf{v} ds = - \int_{\Gamma} \nabla_{\Gamma} u \cdot \mathbf{v} ds. \quad (2.21)$$

Using (2.20)–(2.21) and taking the limit $x_3 \rightarrow 0+$, we obtain the following transparent boundary condition (TBC):

$$\hat{\mathbf{z}} \times (\nabla_{\mathbf{x}} \times \mathbf{E}) = \mathcal{F}(\mathbf{E}) + \mathbf{g} \quad \text{on } \Gamma, \quad (2.22)$$

where $\mathbf{g} = \hat{\mathbf{z}} \times (\nabla_{\mathbf{x}} \times \mathbf{E}^{\text{inc}}) + \hat{\mathbf{z}} \times (\nabla_{\mathbf{x}} \times \mathbf{E}^{\text{ref}})$ and

$$\mathcal{F}(\mathbf{E}) = -2\kappa_0^2 \hat{\mathbf{z}} \times \int_{\Gamma} (\hat{\mathbf{z}} \times \mathbf{E}(\mathbf{y})) g(\mathbf{x}, \mathbf{y}) ds_{\mathbf{y}} - 2\hat{\mathbf{z}} \times \left(\nabla_{\mathbf{x}} \int_{\Gamma} \operatorname{div}_{\Gamma} (\hat{\mathbf{z}} \times \mathbf{E}(\mathbf{y})) g(\mathbf{x}, \mathbf{y}) ds_{\mathbf{y}} \right).$$

Then, by eliminating the magnetic field in (2.1) and using the TBC (2.22), the scattering problem (2.1)–(2.2) can be reduced to an equivalent boundary value problem in the cavity D :

$$\begin{cases} \nabla \times (\nabla \times \mathbf{E}) - \kappa_0^2 \mathbf{E} = 0 & \text{in } D, \\ \boldsymbol{\nu} \times \mathbf{E} = 0 & \text{on } S, \\ \hat{\mathbf{z}} \times (\nabla_{\mathbf{x}} \times \mathbf{E}) = \mathcal{F}(\mathbf{E}) + \mathbf{g} & \text{on } \Gamma. \end{cases} \quad (2.23)$$

3. DISCRETIZATION AND FAST ALGORITHM

In this section, we present the numerical discretization to the Maxwell equation and the TBC, and a fast algorithm for the resulting system.

Let $\mathbf{E} = (E_1, E_2, E_3)$. On the plane surfaces $x_1 = 0$ and $x_1 = a$, the unit outward normal vectors are $(-1, 0, 0)$ and $(1, 0, 0)$, respectively. Using the boundary condition in (2.23), we get the homogeneous Dirichlet boundary condition for E_2 and E_3 :

$$E_2(0, x_2, x_3) = E_2(a, x_2, x_3), \quad E_3(0, x_2, x_3) = E_3(a, x_2, x_3). \quad (3.1)$$

Recall the divergence free condition on the surface:

$$\nabla \cdot \mathbf{E} = \partial_{x_1} E_1 + \partial_{x_2} E_2 + \partial_{x_3} E_3 = 0,$$

which, together with (3.1), implies the homogeneous Neumann boundary condition for E_1 :

$$\partial_{x_1} E_1(0, x_2, x_3) = \partial_{x_1} E_1(a, x_2, x_3) = 0. \quad (3.2)$$

Similarly, on the plane surfaces $x_2 = 0$ and $x_2 = b$, the unit outward normal vectors are $(0, -1, 0)$ and $(0, 1, 0)$, respectively. Using the boundary condition in (2.23), we have the homogeneous Dirichlet boundary condition for E_1 and E_3 :

$$E_1(x_1, 0, x_3) = E_1(x_1, b, x_3), \quad E_3(x_1, 0, x_3) = E_3(x_1, b, x_3). \quad (3.3)$$

Using (3.3) and the divergence free condition again gives the homogeneous Neumann boundary condition for E_2 :

$$\partial_{x_2} E_2(x_1, 0, x_3) = \partial_{x_2} E_2(x_1, b, x_3) = 0. \quad (3.4)$$

By the boundary conditions (3.1)–(3.4), it is easy to show that $E_j, j = 1, 2, 3$ admits the following Fourier series expansions:

$$\begin{cases} E_1(x_1, x_2, x_3) = \sum_{k \in \mathbb{N}^2} E_1^{(k)}(x_3) \cos\left(\frac{k_1 \pi x_1}{a}\right) \sin\left(\frac{k_2 \pi x_2}{b}\right), \\ E_2(x_1, x_2, x_3) = \sum_{k \in \mathbb{N}^2} E_2^{(k)}(x_3) \sin\left(\frac{k_1 \pi x_1}{a}\right) \cos\left(\frac{k_2 \pi x_2}{b}\right), \\ E_3(x_1, x_2, x_3) = \sum_{k \in \mathbb{N}^2} E_3^{(k)}(x_3) \sin\left(\frac{k_1 \pi x_1}{a}\right) \sin\left(\frac{k_2 \pi x_2}{b}\right), \end{cases} \quad (3.5)$$

where $k = (k_1, k_2) \in \mathbb{N}^2$.

By the vector identity $\nabla \times (\nabla \times \mathbf{E}) = -\Delta \mathbf{E} + \nabla(\nabla \cdot \mathbf{E})$ and the divergence free condition $\nabla \cdot \mathbf{E} = 0$, the Maxwell equation in (2.23) can be reduced to the vector Helmholtz equation

$$\Delta \mathbf{E} + \kappa_0^2 \mathbf{E} = 0 \quad \text{in } D. \quad (3.6)$$

Using the boundary condition in (2.23) and the divergence free condition on the plane surfaces $x_3 = -c$, we get the homogeneous Dirichlet boundary condition

$$E_1(x_1, x_2, -c) = E_2(x_1, x_2, -c) = 0 \quad (3.7)$$

and the homogeneous Neumann boundary condition

$$\partial_{x_3} E_3(x_1, x_2, -c) = 0. \quad (3.8)$$

Substituting (3.5) into (3.6)–(3.8), we may get the second order ordinary differential equations for the Fourier coefficients $E_l^{(m,n)}, l = 1, 2$:

$$\begin{cases} \frac{d^2}{dx_3^2} E_l^{(m,n)}(x_3) + \left(\kappa_0^2 - \left(\frac{m\pi}{a}\right)^2 - \left(\frac{n\pi}{b}\right)^2 \right) E_l^{(m,n)}(x_3) = 0, & x_3 \in (-c, 0), \\ E_l^{(m,n)}(-c) = 0, \end{cases} \quad (3.9)$$

where $(m, n) \in \mathbb{N}_l^2$, and the second order ordinary differential equations for the Fourier coefficients $E_3^{(m,n)}$:

$$\begin{cases} \frac{d^2}{dx_3^2} E_3^{(m,n)}(x_3) + \left(\kappa_0^2 - \left(\frac{m\pi}{a} \right)^2 - \left(\frac{n\pi}{b} \right)^2 \right) E_3^{(m,n)}(x_3) = 0, & x_3 \in (-c, 0), \\ \frac{d}{dx_3} E_3^{(m,n)}(-c) = 0. \end{cases} \quad (3.10)$$

where $(m, n) \in \mathbb{N}_3^2$. Here $\mathbb{N}_1^2 = \{0, 1, 2, \dots, M\} \times \{1, 2, \dots, N\}$, $\mathbb{N}_2^2 = \{1, 2, \dots, M\} \times \{0, 1, 2, \dots, N\}$ and $\mathbb{N}_3^2 = \{1, 2, \dots, M\} \times \{1, 2, \dots, N\}$, M and N are the finite truncation numbers of the Fourier series.

Let $\{x_3^j\}_{j=0}^{J+1}$ be a set of uniformly distributed grid points of $[-c, 0]$ with $x_3^{j+1} - x_3^j = h$. Let $E_{l,j}^{(m,n)}$ be the finite difference solution of $E_l^{(m,n)}(x_3)$, $l = 1, 2, 3$ at the point $x_3 = x_3^j$. The discrete finite difference systems for (3.9)–(3.10) are

$$\begin{cases} \frac{E_{l,j-1}^{(m,n)} - 2E_{l,j}^{(m,n)} + E_{l,j+1}^{(m,n)}}{h^2} + \left(\kappa_0^2 - \left(\frac{m\pi}{a} \right)^2 - \left(\frac{n\pi}{b} \right)^2 \right) E_{l,j}^{(m,n)} = 0, & j = 1, 2, \dots, J, \\ E_{l,0}^{(m,n)} = 0, \end{cases}$$

and

$$\begin{cases} \frac{E_{3,j-1}^{(m,n)} - 2E_{3,j}^{(m,n)} + E_{3,j+1}^{(m,n)}}{h^2} + \left(\kappa_0^2 - \left(\frac{m\pi}{a} \right)^2 - \left(\frac{n\pi}{b} \right)^2 \right) E_{3,j}^{(m,n)} = 0, & j = 1, 2, \dots, J, \\ E_{3,1}^{(m,n)} = E_{3,0}^{(m,n)}. \end{cases}$$

The above discrete systems can be written in the matrix form

$$(\mathbf{A}_1 + \mathbf{D}^{(m,n)}) \mathbf{E}_l^{(m,n)} + \mathbf{a}_J E_{l,J+1}^{(m,n)} = 0, \quad (m, n) \in \mathbb{N}_l^2, l = 1, 2, \quad (3.11)$$

and

$$(\mathbf{A}_2 + \mathbf{D}^{(m,n)}) \mathbf{E}_3^{(m,n)} + \mathbf{a}_J E_{3,J+1}^{(m,n)} = 0, \quad (m, n) \in \mathbb{N}_3^2, \quad (3.12)$$

where the vectors of unknowns $\mathbf{E}_l^{(m,n)} = (E_{l,1}^{(m,n)}, E_{l,2}^{(m,n)}, \dots, E_{l,J}^{(m,n)})^\top$, $l = 1, 2, 3$,

$$\mathbf{A}_1 = \begin{pmatrix} -2 & 1 & & \\ 1 & -2 & 1 & \\ & \ddots & \ddots & \ddots \\ & & & 1 & -2 \end{pmatrix}, \quad \mathbf{A}_2 = \begin{pmatrix} -1 & 1 & & \\ 1 & -2 & 1 & \\ & \ddots & \ddots & \ddots \\ & & & 1 & -2 \end{pmatrix}, \quad \mathbf{a}_J = \begin{pmatrix} 0 \\ \vdots \\ 0 \end{pmatrix},$$

and

$$\mathbf{D}^{(m,n)} = h^2 \left(\kappa_0^2 - \left(\frac{m\pi}{a} \right)^2 - \left(\frac{n\pi}{b} \right)^2 \right) \mathbf{I}_J,$$

Here \mathbf{I}_J is the $J \times J$ identity matrix.

Next, we discuss the discretization of the transparent boundary condition (2.22). A simple calculation from the first component of (2.22) yields

$$\begin{aligned} \frac{\partial E_3}{\partial x_1} - \frac{\partial E_1}{\partial x_3} &= 2(i\alpha_1 p_3 + i\beta p_1) e^{i(\alpha_1 x_1 + \alpha_2 x_2)} + 2\kappa_0^2 \int_{\Gamma} E_1(\mathbf{y}) g(\mathbf{x}, \mathbf{y}) ds_{\mathbf{y}} \\ &+ 2 \int_{\Gamma} (-\partial_{y_1} E_2(\mathbf{y}) + \partial_{y_2} E_1(\mathbf{y})) \partial_{x_2} g(\mathbf{x}, \mathbf{y}) ds_{\mathbf{y}}. \end{aligned} \quad (3.13)$$

Substituting (3.5) into (3.13), we have

$$\begin{aligned}
& \sum_{k \in \mathbb{N}_3^2} E_3^{(k)}(0) \frac{k_1 \pi}{a} \cos\left(\frac{k_1 \pi x_1}{a}\right) \sin\left(\frac{k_2 \pi x_2}{b}\right) - \sum_{k \in \mathbb{N}_1^2} \frac{dE_1^{(k)}(0)}{dx_3} \cos\left(\frac{k_1 \pi x_1}{a}\right) \sin\left(\frac{k_2 \pi x_2}{b}\right) \\
&= 2(i\alpha_1 p_3 + i\beta p_1) e^{i(\alpha_1 x_1 + \alpha_2 x_2)} \\
&+ 2\kappa_0^2 \sum_{k \in \mathbb{N}_1^2} E_1^{(k)}(0) \int_{\Gamma} \cos\left(\frac{k_1 \pi y_1}{a}\right) \sin\left(\frac{k_2 \pi y_2}{b}\right) g(\mathbf{x}, \mathbf{y}) ds_{\mathbf{y}} \\
&- 2 \sum_{k \in \mathbb{N}_2^2} E_2^{(k)}(0) \frac{k_1 \pi}{a} \int_{\Gamma} \cos\left(\frac{k_1 \pi y_1}{a}\right) \cos\left(\frac{k_2 \pi y_2}{b}\right) \partial_{x_2} g(\mathbf{x}, \mathbf{y}) ds_{\mathbf{y}} \\
&+ 2 \sum_{k \in \mathbb{N}_1^2} E_1^{(k)}(0) \frac{k_2 \pi}{b} \int_{\Gamma} \cos\left(\frac{k_1 \pi y_1}{a}\right) \cos\left(\frac{k_2 \pi y_2}{b}\right) \partial_{x_2} g(\mathbf{x}, \mathbf{y}) ds_{\mathbf{y}}. \tag{3.14}
\end{aligned}$$

Multiplying both sides of (3.14) by $\cos\left(\frac{m\pi x_1}{a}\right) \sin\left(\frac{n\pi x_2}{b}\right)$, $(m, n) \in \mathbb{N}_1^2$ and integrating over Γ , we obtain

$$\begin{aligned}
E_3^{(m,n)}(0) p^{(m,n)} - \frac{dE_1^{(m,n)}(0)}{dx_3} q^{(m,n)} &= 2(i\alpha_1 p_3 + i\beta p_1) \tilde{g}_1^{(m,n)} + 2\kappa_0^2 \sum_{k \in \mathbb{N}_1^2} E_1^{(k)}(0) \tilde{F}_{1,(k)}^{(m,n)} \\
&- 2 \sum_{k \in \mathbb{N}_2^2} E_2^{(k)}(0) \frac{k_1 \pi}{a} \tilde{G}_{1,(k)}^{(m,n)} + 2 \sum_{k \in \mathbb{N}_1^2} E_1^{(k)}(0) \frac{k_2 \pi}{b} \tilde{H}_{1,(k)}^{(m,n)},
\end{aligned}$$

where

$$p^{(m,n)} = \begin{cases} 0, & \text{if } m = 0, \\ \frac{bm\pi}{4}, & \text{others,} \end{cases} \quad q^{(m,n)} = \begin{cases} \frac{ab}{2}, & \text{if } m = 0, \\ \frac{ab}{4}, & \text{others,} \end{cases}$$

and

$$\tilde{g}_1^{(m,n)} = \int_{\Gamma} \cos\left(\frac{m\pi x_1}{a}\right) \sin\left(\frac{n\pi x_2}{b}\right) e^{i(\alpha_1 x_1 + \alpha_2 x_2)} ds_{\mathbf{x}}, \tag{3.15}$$

$$\tilde{F}_{1,(k)}^{(m,n)} = \int_{\Gamma} \cos\left(\frac{m\pi x_1}{a}\right) \sin\left(\frac{n\pi x_2}{b}\right) \left(\int_{\Gamma} \cos\left(\frac{k_1 \pi y_1}{a}\right) \sin\left(\frac{k_2 \pi y_2}{b}\right) g(\mathbf{x}, \mathbf{y}) ds_{\mathbf{y}} \right) ds_{\mathbf{x}}, \tag{3.16}$$

$$\tilde{G}_{1,(k)}^{(m,n)} = \int_{\Gamma} \cos\left(\frac{m\pi x_1}{a}\right) \sin\left(\frac{n\pi x_2}{b}\right) \left(\int_{\Gamma} \cos\left(\frac{k_1 \pi y_1}{a}\right) \cos\left(\frac{k_2 \pi y_2}{b}\right) \partial_{x_2} g(\mathbf{x}, \mathbf{y}) ds_{\mathbf{y}} \right) ds_{\mathbf{x}}, \tag{3.17}$$

$$\tilde{H}_{1,(k)}^{(m,n)} = \int_{\Gamma} \cos\left(\frac{m\pi x_1}{a}\right) \sin\left(\frac{n\pi x_2}{b}\right) \left(\int_{\Gamma} \cos\left(\frac{k_1 \pi y_1}{a}\right) \cos\left(\frac{k_2 \pi y_2}{b}\right) \partial_{x_2} g(\mathbf{x}, \mathbf{y}) ds_{\mathbf{y}} \right) ds_{\mathbf{x}}. \tag{3.18}$$

By using a backward finite difference scheme for the normal derivative and the fact that $E_{l,J+1}^{(k)} = E_l^{(k)}(0)$, $l = 1, 2, 3$, we get

$$\begin{aligned}
E_{3,J+1}^{(m,n)} p^{(m,n)} - \frac{E_{1,J+1}^{(m,n)} - E_{1,J}^{(m,n)}}{h} q^{(m,n)} &= 2(i\alpha_1 p_3 + i\beta p_1) \tilde{g}_1^{(m,n)} + 2\kappa_0^2 \sum_{k \in \mathbb{N}_1^2} E_{1,J+1}^{(k)} \tilde{F}_{1,(k)}^{(m,n)} \\
&- 2 \sum_{k \in \mathbb{N}_2^2} E_{2,J+1}^{(k)} \left(\frac{k_1 \pi}{a} \right) \tilde{G}_{1,(k)}^{(m,n)} + 2 \sum_{k \in \mathbb{N}_1^2} E_{1,J+1}^{(k)} \left(\frac{k_2 \pi}{b} \right) \tilde{H}_{1,(k)}^{(m,n)}. \tag{3.19}
\end{aligned}$$

For $(m, n) \in \mathbb{N}_1^2$, we define the following notations:

$$\begin{aligned} g_1^{(m,n)} &:= \frac{h}{q^{(m,n)}} 2(i\alpha_1 p_3 + i\beta p_1) \tilde{g}_1^{(m,n)}, \\ F_{1,(k)}^{(m,n)} &:= \frac{h}{q^{(m,n)}} 2\kappa_0^2 \tilde{F}_{1,(k)}^{(m,n)}, \\ G_{1,(k)}^{(m,n)} &:= \frac{h}{q^{(m,n)}} \frac{-2k_1\pi}{a} \tilde{G}_{1,(k)}^{(m,n)}, \\ H_{1,(k)}^{(m,n)} &:= \frac{h}{q^{(m,n)}} \frac{2k_2\pi}{b} \tilde{H}_{1,(k)}^{(m,n)}. \end{aligned}$$

Thus, we obtain from (3.19) that

$$\begin{aligned} E_{3,J+1}^{(m,n)} \frac{p^{(m,n)} h}{q^{(m,n)}} - E_{1,J+1}^{(m,n)} + E_{1,J}^{(m,n)} - \sum_{k \in \mathbb{N}_1^2} E_{1,J+1}^{(k)} F_{1,(k)}^{(m,n)} \\ - \sum_{k \in \mathbb{N}_2^2} E_{2,J+1}^{(k)} G_{1,(k)}^{(m,n)} - \sum_{k \in \mathbb{N}_1^2} E_{1,J+1}^{(k)} H_{1,(k)}^{(m,n)} = g_1^{(m,n)}, \quad (m, n) \in \mathbb{N}_1^2, \end{aligned}$$

which can be written in a matrix form

$$\hat{\mathbf{I}}_1 \mathbf{E}_{1,J} + (-\hat{\mathbf{I}}_1 - \mathbf{F}_1 - \mathbf{H}_1) \mathbf{E}_{1,J+1} - \mathbf{G}_1 \mathbf{E}_{2,J+1} + \mathbf{I}_1 \mathbf{E}_{3,J+1} = \mathbf{g}_1. \quad (3.20)$$

Here $\hat{\mathbf{I}}_1 = \mathbf{I}_{((M+1)N)}$, $\mathbf{I}_1 = \tilde{\mathbf{I}}_1 \otimes \mathbf{I}_N$, \otimes denotes the Kronecker product, and

$$\tilde{\mathbf{I}}_1 = \begin{pmatrix} 0 & \cdots & 0 \\ \frac{\pi h}{a} & & \\ & \ddots & \\ & & \frac{M\pi h}{a} \end{pmatrix}.$$

For clarity, we refer to Appendix A for the entries of \mathbf{F}_1 , \mathbf{H}_1 , \mathbf{G}_1 , \mathbf{g}_1 , and $\mathbf{E}_{l,j}$ for $l = 1, 2, 3, 0 \leq j \leq J+1$.

Similarly, the second component of TBC (2.22) can be discretized as

$$\hat{\mathbf{I}}_2 \mathbf{E}_{2,J} - \mathbf{H}_2 \mathbf{E}_{1,J+1} + (-\hat{\mathbf{I}}_2 - \mathbf{F}_2 - \mathbf{G}_2) \mathbf{E}_{2,J+1} + \mathbf{I}_2 \mathbf{E}_{3,J+1} = \mathbf{g}_2, \quad (3.21)$$

where $\hat{\mathbf{I}}_2 = \mathbf{I}_{(M(N+1))}$, $\mathbf{I}_2 = \mathbf{I}_M \otimes \tilde{\mathbf{I}}_2$, and

$$\tilde{\mathbf{I}}_2 = \begin{pmatrix} 0 & \cdots & 0 \\ \frac{\pi h}{b} & & \\ & \ddots & \\ & & \frac{N\pi h}{b} \end{pmatrix}_{(N+1) \times N}.$$

Again, the entries of the vectors \mathbf{F}_2 , \mathbf{H}_2 , \mathbf{G}_2 and \mathbf{g}_2 can be found in Appendix A.

Recall the divergence free condition on the surface Γ ,

$$\partial_{x_1} E_1 + \partial_{x_2} E_2 + \partial_{x_3} E_3 = 0. \quad (3.22)$$

Substituting (3.5) into (3.22), we have

$$\begin{aligned} \sum_{k \in \mathbb{N}_1^2} E_1^{(k)}(0) \left(\frac{-k_1\pi}{a} \right) \sin \left(\frac{k_1\pi x_1}{a} \right) \sin \left(\frac{k_2\pi x_2}{b} \right) + \sum_{k \in \mathbb{N}_2^2} E_2^{(k)}(0) \left(\frac{-k_2\pi}{b} \right) \sin \left(\frac{k_1\pi x_1}{a} \right) \sin \left(\frac{k_2\pi x_2}{b} \right) \\ + \sum_{k \in \mathbb{N}_3^2} \frac{\partial E_3^{(k)}(0)}{\partial x_3} \sin \left(\frac{k_1\pi x_1}{a} \right) \sin \left(\frac{k_2\pi x_2}{b} \right) = 0. \end{aligned} \quad (3.23)$$

Multiplying both side of (3.23) by $\sin(\frac{m\pi x_1}{a})\sin(\frac{n\pi x_2}{b})$, $(m, n) \in \mathbb{N}_3^2$, integrating over Γ , and using the orthogonality of the trigonometric functions, we obtain

$$\left(\frac{-m\pi ab}{a} \frac{1}{4}\right) E_1^{(m,n)}(0) + \left(\frac{-n\pi ab}{b} \frac{1}{4}\right) E_2^{(m,n)}(0) + \left(\frac{ab}{4}\right) \frac{\partial E_3^{(m,n)}(0)}{\partial x_3} = 0. \quad (3.24)$$

By using a backward finite difference scheme, we get

$$E_{3,J}^{(m,n)} + \left(\frac{m\pi}{a}\right) E_{1,J+1}^{(m,n)} + \left(\frac{n\pi}{b}\right) E_{2,J+1}^{(m,n)} - E_{3,J+1}^{(m,n)} = 0. \quad (3.25)$$

Let

$$\tilde{\mathbf{I}}_3 = \begin{pmatrix} 0 & \frac{\pi h}{a} & & \\ \vdots & & \ddots & \\ 0 & & & \frac{M\pi h}{a} \end{pmatrix}, \quad \tilde{\mathbf{I}}_4 = \begin{pmatrix} 0 & \frac{\pi h}{b} & & \\ \vdots & & \ddots & \\ 0 & & & \frac{N\pi h}{b} \end{pmatrix},$$

$\mathbf{F}_3 = \tilde{\mathbf{I}}_3 \otimes \mathbf{I}_N$ and $\mathbf{G}_3 = \mathbf{I}_M \otimes \tilde{\mathbf{I}}_4$. The discrete system (3.25) can be rewritten as

$$\hat{\mathbf{I}}_3 \mathbf{E}_{3,J} + \mathbf{F}_3 \mathbf{E}_{1,J+1} + \mathbf{G}_3 \mathbf{E}_{2,J+1} - \hat{\mathbf{I}}_3 \mathbf{E}_{3,J+1} = 0, \quad (3.26)$$

where $\hat{\mathbf{I}}_3 = \mathbf{I}_{(MN)}$. It follows from (3.20)–(3.21) and (3.26) that

$$\begin{pmatrix} \hat{\mathbf{I}}_1 & & \\ & \hat{\mathbf{I}}_2 & \\ & & \hat{\mathbf{I}}_3 \end{pmatrix} \begin{pmatrix} \mathbf{E}_{1,J} \\ \mathbf{E}_{2,J} \\ \mathbf{E}_{3,J} \end{pmatrix} + \begin{pmatrix} -\hat{\mathbf{I}}_1 - \mathbf{F}_1 - \mathbf{H}_1 & & \\ & -\mathbf{H}_2 & \\ & & \mathbf{F}_3 \end{pmatrix} \begin{pmatrix} -\mathbf{G}_1 & & \mathbf{I}_1 \\ -\hat{\mathbf{I}}_2 - \mathbf{F}_2 - \mathbf{G}_2 & & \mathbf{I}_2 \\ & & \mathbf{G}_3 \\ & & & -\hat{\mathbf{I}}_3 \end{pmatrix} \begin{pmatrix} \mathbf{E}_{1,J+1} \\ \mathbf{E}_{2,J+1} \\ \mathbf{E}_{3,J+1} \end{pmatrix} = \begin{pmatrix} \mathbf{g}_1 \\ \mathbf{g}_2 \\ 0 \end{pmatrix} \quad (3.27)$$

Clearly, the linear systems (3.11)–(3.12) and (3.27) are coupled and give the global system. Next, we use Gaussian elimination method to decouple the global system into a linear system with the unknowns only on the aperture, which may reduce the computational complexity greatly and lead to a fast algorithm.

Let

$$\mathbf{L}_1^{(m,n)} \mathbf{U}_1^{(m,n)} = \mathbf{A}_1 + \mathbf{D}^{(m,n)}, \quad (m, n) \in \mathbb{N}_l^2, \quad l = 1, 2, \quad (3.28)$$

and

$$\mathbf{L}_2^{(m,n)} \mathbf{U}_2^{(m,n)} = \mathbf{A}_2 + \mathbf{D}^{(m,n)}, \quad (m, n) \in \mathbb{N}_3^2, \quad (3.29)$$

be the LU-decomposition, where $\mathbf{A}_1 + \mathbf{D}^{(m,n)}$ and $\mathbf{A}_2 + \mathbf{D}^{(m,n)}$ are the symmetric tridiagonal matrices in (3.11) and (3.12), respectively. Since $\mathbf{L}_1^{(m,n)}$ and $\mathbf{L}_2^{(m,n)}$ are nonsingular, we obtain

$$\mathbf{U}_1^{(m,n)} \mathbf{E}_l^{(m,n)} + (\mathbf{L}_1^{(m,n)})^{-1} \mathbf{a}_{J+1} \mathbf{E}_{l,J+1}^{(m,n)} = 0, \quad (m, n) \in \mathbb{N}_l^2, \quad l = 1, 2, \quad (3.30)$$

$$\mathbf{U}_2^{(m,n)} \mathbf{E}_3^{(m,n)} + (\mathbf{L}_2^{(m,n)})^{-1} \mathbf{a}_{J+1} \mathbf{E}_{3,J+1}^{(m,n)} = 0, \quad (m, n) \in \mathbb{N}_3^2, \quad (3.31)$$

where $\mathbf{U}_1^{(m,n)} = (r_{1,(pq)}^{m,n})$ and $\mathbf{U}_2^{(m,n)} = (r_{2,(pq)}^{m,n})$.

Combining the last equations of the systems (3.30) and (3.31) gives

$$\begin{pmatrix} \mathbf{R}_1 & & \\ & \mathbf{R}_2 & \\ & & \mathbf{R}_3 \end{pmatrix} \begin{pmatrix} \mathbf{E}_{1,J} \\ \mathbf{E}_{2,J} \\ \mathbf{E}_{3,J} \end{pmatrix} + \begin{pmatrix} \hat{\mathbf{I}}_1 & & \\ & \hat{\mathbf{I}}_2 & \\ & & \hat{\mathbf{I}}_3 \end{pmatrix} \begin{pmatrix} \mathbf{E}_{1,J+1} \\ \mathbf{E}_{2,J+1} \\ \mathbf{E}_{3,J+1} \end{pmatrix} = 0, \quad (3.32)$$

where

$$\mathbf{R}_l = \text{diag}(r_{1,(JJ)}^{(m,n)}), \quad (m, n) \in \mathbb{N}_l^2, \quad l = 1, 2,$$

$$\mathbf{R}_3 = \text{diag}(r_{2,(JJ)}^{(m,n)}), \quad (m, n) \in \mathbb{N}_3^2.$$

If κ_0^2 is not an eigenvalue of the Helmholtz operator with Dirichlet boundary condition, the continuous Helmholtz problem admits a unique solution; for h small enough, as an approximate problem, the discrete Helmholtz problem can also be shown to have a unique solution [23], which implies that

$$r_{1,(JJ)}^{(m,n)} \neq 0, \quad (m, n) \in \mathbb{N}_l^2, \quad l = 1, 2, \quad (3.33)$$

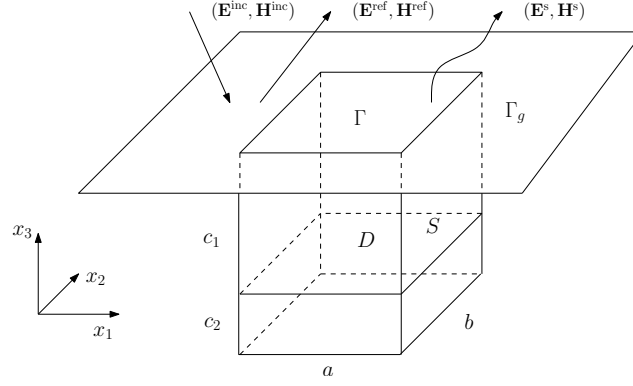


FIGURE 2. The problem geometry of the electromagnetic scattering by a rectangular cavity filled with a layered medium.

and

$$r_{2,(JJ)}^{(m,n)} \neq 0, \quad (m, n) \in \mathbb{N}_3^2. \quad (3.34)$$

Consequently, combining (3.32) and (3.27) yields

$$\begin{pmatrix} -\hat{\mathbf{I}}_1 - \mathbf{F}_1 - \mathbf{H}_1 - \mathbf{R}_1^{-1} & -\mathbf{G}_1 & \mathbf{I}_1 \\ -\mathbf{H}_2 & -\hat{\mathbf{I}}_2 - \mathbf{F}_2 - \mathbf{G}_2 - \mathbf{R}_2^{-1} & \mathbf{I}_2 \\ \mathbf{F}_3 & \mathbf{G}_3 & -\hat{\mathbf{I}}_3 - \mathbf{R}_3^{-1} \end{pmatrix} \begin{pmatrix} \mathbf{E}_{1,J+1} \\ \mathbf{E}_{2,J+1} \\ \mathbf{E}_{3,J+1} \end{pmatrix} = \begin{pmatrix} \mathbf{g}_1 \\ \mathbf{g}_2 \\ 0 \end{pmatrix}. \quad (3.35)$$

Solving the linear system (3.35) gives the solution $E_{l,J+1}, l = 1, 2, 3$ on the interface Γ . The rest of the unknowns can be simply obtained by solving the following systems:

$$\begin{aligned} (\mathbf{A}_1 + \mathbf{D}^{(m,n)}) \mathbf{E}_l^{(m,n)} &= -\mathbf{a}_{J+1} E_{l,J+1}^{(m,n)}, \quad l = 1, 2, \\ (\mathbf{A}_2 + \mathbf{D}^{(m,n)}) \mathbf{E}_3^{(m,n)} &= -\mathbf{a}_{J+1} E_{3,J+1}^{(m,n)}. \end{aligned} \quad (3.36)$$

Remark 3.1. Since the medium is assumed to be homogeneous in the cavity, it follows from the Maxwell equation (2.23) that the electrical field \mathbf{E} is divergence free in D . Although the solutions are solved separately in D , they admit the series expansions (3.5) and satisfy the divergence free condition due to (2.23).

4. LAYERED MEDIA

This section is devoted to the numerical solution of the electromagnetic scattering by an open cavity with a layered medium. Specifically, we assume that the cavity is filled with a multi-layered medium, which is characterized by the piecewise constant dielectric permittivity $\varepsilon_l, l = 1, 2, \dots, L$. The medium is still assumed to be nonmagnetic with a constant magnetic permeability $\mu = \mu_0$ everywhere and has a constant dielectric permittivity $\varepsilon = \varepsilon_0$ in the upper half space. Without loss of generality, we discuss a two-layered medium in D . Denote by c_1 and c_2 the depth of the two layer domain D_1 and D_2 , respectively. The problem geometry is depicted in Figure 2. The open aperture of the cavity $\Gamma = [0, a] \times [0, b]$ and the total depth of the cavity is c , i.e., $c = c_1 + c_2$.

Let $\mathbf{E}_1 = (u_1, u_2, u_3)$ and $\mathbf{E}_2 = (v_1, v_2, v_3)$ be the total electric field in domain D_1 and D_2 , respectively. Similar to the homogeneous case, it can be shown from the boundary condition and

divergence free condition that u_j and $v_j, j = 1, 2, 3$ admit the following Fourier series expansions:

$$\begin{cases} u_1(x_1, x_2, x_3) = \sum_{k \in \mathbb{N}^2} u_1^{(k)}(x_3) \cos\left(\frac{k_1 \pi x_1}{a}\right) \sin\left(\frac{k_2 \pi x_2}{b}\right), \\ u_2(x_1, x_2, x_3) = \sum_{k \in \mathbb{N}^2} u_2^{(k)}(x_3) \sin\left(\frac{k_1 \pi x_1}{a}\right) \cos\left(\frac{k_2 \pi x_2}{b}\right), \\ u_3(x_1, x_2, x_3) = \sum_{k \in \mathbb{N}^2} u_3^{(k)}(x_3) \sin\left(\frac{k_1 \pi x_1}{a}\right) \sin\left(\frac{k_2 \pi x_2}{b}\right), \end{cases} \quad (4.1)$$

and

$$\begin{cases} v_1(x_1, x_2, x_3) = \sum_{k \in \mathbb{N}^2} v_1^{(k)}(x_3) \cos\left(\frac{k_1 \pi x_1}{a}\right) \sin\left(\frac{k_2 \pi x_2}{b}\right), \\ v_2(x_1, x_2, x_3) = \sum_{k \in \mathbb{N}^2} v_2^{(k)}(x_3) \sin\left(\frac{k_1 \pi x_1}{a}\right) \cos\left(\frac{k_2 \pi x_2}{b}\right), \\ v_3(x_1, x_2, x_3) = \sum_{k \in \mathbb{N}^2} v_3^{(k)}(x_3) \sin\left(\frac{k_1 \pi x_1}{a}\right) \sin\left(\frac{k_2 \pi x_2}{b}\right), \end{cases} \quad (4.2)$$

where $k = (k_1, k_2) \in \mathbb{N}^2$.

In the lower part of the layered medium D_2 , the electric field $\mathbf{E}_2 = (v_1, v_2, v_3)$ satisfies the Helmholtz equation

$$\Delta \mathbf{E}_2 + \kappa_2^2 \mathbf{E}_2 = 0 \quad \text{in } D_2, \quad (4.3)$$

the homogeneous Dirichlet boundary condition

$$v_1(x_1, x_2, -c) = v_2(x_1, x_2, -c) = 0, \quad (4.4)$$

and the homogeneous Neumann boundary condition

$$\partial_{x_3} v_3(x_1, x_2, -c) = 0, \quad (4.5)$$

where $\kappa_2 = \omega \sqrt{\varepsilon_2 \mu}$ is the wavenumber in D_2 .

Substituting (4.2) into (4.3)–(4.5), we get the second order ordinary differential equations with the homogeneous Dirichlet boundary condition at $x_3 = -c$ for the Fourier coefficients $v_l^{(m,n)}, l = 1, 2$:

$$\begin{cases} \frac{d^2}{dx_3^2} v_l^{(m,n)}(x_3) + \left(\kappa_2^2 - \left(\frac{m\pi}{a}\right)^2 - \left(\frac{n\pi}{b}\right)^2 \right) v_l^{(m,n)}(x_3) = 0, & x_3 \in (-c, -c_1), \\ v_l^{(m,n)}(-c) = 0, \end{cases} \quad (4.6)$$

where $(m, n) \in \mathbb{N}_l^2$, and the second order ordinary differential equations with the homogeneous Neumann boundary condition at $x_3 = -c$ for the Fourier coefficients $v_3^{(m,n)}$:

$$\begin{cases} \frac{d^2}{dx_3^2} v_3^{(m,n)}(x_3) + \left(\kappa_2^2 - \left(\frac{m\pi}{a}\right)^2 - \left(\frac{n\pi}{b}\right)^2 \right) v_3^{(m,n)}(x_3) = 0, & x_3 \in (-c, -c_1), \\ \frac{d}{dx_3} v_3^{(m,n)}(-c) = 0. \end{cases} \quad (4.7)$$

where $(m, n) \in \mathbb{N}_3^2$.

Define by $\{x_3^j\}_{j=0}^{J+1}$ a set of uniformly distributed grid points in $[-c, -c_1]$, where $h = x_3^{j+1} - x_3^j$. Let $v_{l,j}^{(m,n)}, l = 1, 2, 3$ be the finite difference solution of $v_l^{(m,n)}(x_3)$ at the point $x_3 = x_3^j$. Similar to the discretization of (3.9)–(3.10), the discrete system of (4.6)–(4.7) can be written in the matrix form

$$(\mathbf{A}_1 + \mathbf{D}_2^{(m,n)}) \mathbf{v}_l^{(m,n)} + \mathbf{a}_J v_{l,J+1}^{(m,n)} = 0, \quad (m, n) \in \mathbb{N}_l^2, l = 1, 2, \quad (4.8)$$

and

$$(\mathbf{A}_2 + \mathbf{D}_2^{(m,n)})\mathbf{v}_3^{(m,n)} + \mathbf{a}_J v_{3,J+1}^{(m,n)} = 0, \quad (m, n) \in \mathbb{N}_3^2, \quad (4.9)$$

where the vector of unknowns $\mathbf{v}_l^{(m,n)} = (v_{l,1}^{(m,n)}, v_{l,2}^{(m,n)}, \dots, v_{l,J}^{(m,n)})^\top$, $l = 1, 2, 3$,

$$\mathbf{A}_1 = \begin{pmatrix} -2 & 1 & & & \\ 1 & -2 & 1 & & \\ & \ddots & \ddots & \ddots & \\ & & & 1 & -2 \end{pmatrix}, \quad \mathbf{A}_2 = \begin{pmatrix} -1 & 1 & & & \\ 1 & -2 & 1 & & \\ & \ddots & \ddots & \ddots & \\ & & & 1 & -2 \end{pmatrix}, \quad \mathbf{a}_J = \begin{pmatrix} 0 \\ \vdots \\ 0 \\ 1 \end{pmatrix},$$

and

$$\mathbf{D}_2^{(m,n)} = h^2 \left(\kappa_2^2 - \left(\frac{m\pi}{a} \right)^2 - \left(\frac{n\pi}{b} \right)^2 \right) \mathbf{I}_J,$$

Again, we apply the Gaussian elimination method to solve the linear system (4.8)–(4.9). Let

$$\mathbf{L}_1^{(m,n)} \mathbf{U}_1^{(m,n)} = \mathbf{A}_1 + \mathbf{D}_2^{(m,n)}, \quad (m, n) \in \mathbb{N}_l^2, \quad l = 1, 2, \quad (4.10)$$

and

$$\mathbf{L}_2^{(m,n)} \mathbf{U}_2^{(m,n)} = \mathbf{A}_2 + \mathbf{D}_2^{(m,n)}, \quad (m, n) \in \mathbb{N}_3^2, \quad (4.11)$$

be the LU-decomposition, where $\mathbf{U}_1^{(m,n)} = (r_{1,(pq)}^{(m,n)})$ and $\mathbf{U}_2^{(m,n)} = (r_{2,(pq)}^{(m,n)})$. Since $\mathbf{L}_1^{(m,n)}$ and $\mathbf{L}_2^{(m,n)}$ are nonsingular, we obtain

$$\mathbf{U}_1^{(m,n)} \mathbf{v}_l^{(m,n)} + (\mathbf{L}_1^{(m,n)})^{-1} \mathbf{a}_J v_{l,J+1}^{(m,n)} = 0, \quad (m, n) \in \mathbb{N}_l^2, \quad l = 1, 2, \quad (4.12)$$

and

$$\mathbf{U}_2^{(m,n)} \mathbf{v}_3^{(m,n)} + (\mathbf{L}_2^{(m,n)})^{-1} \mathbf{a}_J v_{3,J+1}^{(m,n)} = 0, \quad (m, n) \in \mathbb{N}_3^2. \quad (4.13)$$

Combining the last equations of the systems (4.12) and (4.13) gives

$$r_{1,(JJ)}^{(m,n)} v_{l,J}^{(m,n)} + v_{l,J+1}^{(m,n)} = 0, \quad (m, n) \in \mathbb{N}_l^2, \quad l = 1, 2, \quad (4.14)$$

$$r_{2,(JJ)}^{(m,n)} v_{3,J}^{(m,n)} + v_{3,J+1}^{(m,n)} = 0, \quad (m, n) \in \mathbb{N}_3^2. \quad (4.15)$$

In the upper part of the layered medium D_1 , the electric field $\mathbf{E}_1 = (u_1, u_2, u_3)$ satisfies the Helmholtz equation

$$\Delta \mathbf{E}_1 + \kappa_1^2 \mathbf{E}_1 = 0 \quad \text{in } D_1, \quad (4.16)$$

where $\kappa_1 = \omega \sqrt{\varepsilon_1 \mu}$ is the wavenumber in D_1 . Substituting (4.1) into (4.16) yields

$$\frac{d^2}{dx_3^2} u_l^{(m,n)}(x_3) + \left(\kappa_1^2 - \left(\frac{m\pi}{a} \right)^2 - \left(\frac{n\pi}{b} \right)^2 \right) u_l^{(m,n)}(x_3) = 0, \quad x_3 \in (-c_1, 0), \quad (m, n) \in \mathbb{N}_l^2, \quad (4.17)$$

for $l = 1, 2, 3$.

Let $\{x_3^i\}_{i=0}^{I+1}$ be a set of uniformly distributed grid points in $[-c_1, 0]$ with $x_3^{i+1} - x_3^i = h$. Let $u_{l,i}^{(m,n)}$ be the finite difference solution of $u_l^{(m,n)}(x_3)$, $l = 1, 2, 3$ at the point $x_3 = x_3^i$. The discrete finite difference systems (4.17) can be written as

$$\frac{u_{l,i-1}^{(m,n)} - 2u_{l,i}^{(m,n)} + u_{l,i+1}^{(m,n)}}{h^2} + \left(\kappa_1^2 - \left(\frac{m\pi}{a} \right)^2 - \left(\frac{n\pi}{b} \right)^2 \right) u_{l,i}^{(m,n)} = 0, \quad i = 1, 2, \dots, I, \quad (4.18)$$

where $(m, n) \in \mathbb{N}_l^2$, $l = 1, 2, 3$.

Next, we consider the continuity conditions on $\Gamma_1 = \{\mathbf{x} \in \mathbb{R}^3 | (x_1, x_2) \in [0, a] \times [0, b], x_3 = -c_1\}$. By Maxwell's equations, the tangential traces of the electromagnetic fields are continuous, i.e.,

$$\boldsymbol{\nu} \times \mathbf{E}_1 = \boldsymbol{\nu} \times \mathbf{E}_2, \quad \boldsymbol{\nu} \times \mathbf{H}_1 = \boldsymbol{\nu} \times \mathbf{H}_2,$$

the normal components of the electric and magnetic flux density are continuous, i.e.,

$$\boldsymbol{\nu} \cdot (\varepsilon_1 \mathbf{E}_1) = \boldsymbol{\nu} \cdot (\varepsilon_2 \mathbf{E}_2), \quad \boldsymbol{\nu} \cdot (\mu_0 \mathbf{H}_1) = \boldsymbol{\nu} \cdot (\mu_0 \mathbf{H}_2).$$

In addition, the electric field is divergence free, i.e.,

$$\nabla \cdot \mathbf{E}_1 = \nabla \cdot \mathbf{E}_2 = 0.$$

Componentwisely, the above continuity and divergence free conditions are

$$u_1(x_1, x_2, -c_1) = v_1(x_1, x_2, -c_1), \quad (4.19)$$

$$u_2(x_1, x_2, -c_1) = v_2(x_1, x_2, -c_1), \quad (4.20)$$

$$\varepsilon_1 u_3(x_1, x_2, -c_1) = \varepsilon_2 v_3(x_1, x_2, -c_1), \quad (4.21)$$

$$\partial_{x_1} u_3(x_1, x_2, -c_1) - \partial_{x_3} u_1(x_1, x_2, -c_1) = \partial_{x_1} v_3(x_1, x_2, -c_1) - \partial_{x_3} v_1(x_1, x_2, -c_1), \quad (4.22)$$

$$\partial_{x_2} u_3(x_1, x_2, -c_1) - \partial_{x_3} u_2(x_1, x_2, -c_1) = \partial_{x_2} v_3(x_1, x_2, -c_1) - \partial_{x_3} v_2(x_1, x_2, -c_1), \quad (4.23)$$

$$\partial_{x_3} u_3(x_1, x_2, -c_1) = \partial_{x_3} v_3(x_1, x_2, -c_1). \quad (4.24)$$

Substituting (4.1)–(4.2) into (4.19) and matching the modes for the Fourier series expansions, we obtain

$$u_1^{(m,n)}(-c_1) = v_1^{(m,n)}(-c_1), \quad (m, n) \in \mathbb{N}_1^2,$$

which implies

$$u_{1,0}^{(m,n)} = v_{1,J+1}^{(m,n)}, \quad (m, n) \in \mathbb{N}_1^2. \quad (4.25)$$

Similarly, we have from (4.20)–(4.21) that

$$u_{2,0}^{(m,n)} = v_{2,J+1}^{(m,n)}, \quad (m, n) \in \mathbb{N}_2^2, \quad (4.26)$$

and

$$\varepsilon_1 u_{3,0}^{(m,n)} = \varepsilon_2 v_{3,J+1}^{(m,n)} \quad (m, n) \in \mathbb{N}_3^2. \quad (4.27)$$

Substituting (4.1)–(4.2) into (4.22), multiplying the resulting equation by $\cos(\frac{m\pi x_1}{a})\sin(\frac{n\pi x_2}{b})$, $(m, n) \in \mathbb{N}_1^2$, and integrating over Γ_1 , we obtain from the orthogonality of the trigonometric functions that

$$\frac{\partial u_1^{(0,n)}(-c_1)}{\partial x_3} = \frac{\partial v_1^{(0,n)}(-c_1)}{\partial x_3}, \quad n = 1, 2, \dots, N,$$

and

$$u_3^{(m,n)}(-c_1) \frac{m\pi}{a} - \frac{\partial u_1^{(m,n)}(-c_1)}{\partial x_3} = v_3^{(m,n)}(-c_1) \frac{m\pi}{a} - \frac{\partial v_1^{(m,n)}(-c_1)}{\partial x_3}, \quad (m, n) \in \mathbb{N}_3^2.$$

Using the backward and forward finite difference schemes, we obtain

$$\frac{u_{1,1}^{(0,n)} - u_{1,0}^{(0,n)}}{h} = \frac{v_{1,J+1}^{(0,n)} - v_{1,J}^{(0,n)}}{h}, \quad n = 1, 2, \dots, N, \quad (4.28)$$

and

$$\left(\frac{m\pi}{a}\right) u_{3,0}^{(m,n)} - \frac{u_{1,1}^{(m,n)} - u_{1,0}^{(m,n)}}{h} = \left(\frac{m\pi}{a}\right) v_{3,J+1}^{(m,n)} - \frac{v_{1,J+1}^{(m,n)} - v_{1,J}^{(m,n)}}{h}, \quad (m, n) \in \mathbb{N}_3^2. \quad (4.29)$$

Combining (4.28)–(4.29), (4.14), (4.25) and (4.27) gives

$$\left(-1/r_{1,(JJ)}^{(0,n)} - 2\right) u_{1,0}^{(0,n)} + u_{1,1}^{(0,n)} = 0, \quad n = 1, 2, \dots, N, \quad (4.30)$$

and

$$\left(-1/r_{1,(JJ)}^{(m,n)} - 2\right) u_{1,0}^{(m,n)} + \left(\frac{\varepsilon_1}{\varepsilon_2} - 1\right) \left(\frac{m\pi h}{a}\right) u_{3,0}^{(m,n)} + u_{1,1}^{(m,n)} = 0, \quad (m, n) \in \mathbb{N}_3^2. \quad (4.31)$$

For simplicity, let $u_{3,0}^{(0,n)} = u_{3,I+1}^{(0,n)} = 0$, $n = 1, 2, \dots, N$ and $u_{3,0}^{(m,0)} = u_{3,I+1}^{(m,0)} = 0$, $m = 1, 2, \dots, M$ in the rest of this section. Thus, (4.30)–(4.31) can be written uniformly as

$$\left(-1/r_{1,(JJ)}^{(m,n)} - 2\right) u_{1,0}^{(m,n)} + \left(\frac{\varepsilon_1}{\varepsilon_2} - 1\right) \left(\frac{m\pi h}{a}\right) u_{3,0}^{(m,n)} + u_{1,1}^{(m,n)} = 0, \quad (m, n) \in \mathbb{N}_1^2. \quad (4.32)$$

Similarly, based on the condition (4.23)–(4.24), we get

$$\left(-1/r_{1,(JJ)}^{(m,n)} - 2\right)u_{2,0}^{(m,n)} + \left(\frac{\varepsilon_1}{\varepsilon_2} - 1\right)\left(\frac{n\pi h}{b}\right)u_{3,0}^{(m,n)} + u_{2,1}^{(m,n)} = 0, \quad (m, n) \in \mathbb{N}_2^2, \quad (4.33)$$

and

$$\left(\left(-1/r_{2,(JJ)}^{(m,n)} - 1\right)\frac{\varepsilon_1}{\varepsilon_2} - 1\right)u_{3,0}^{(m,n)} + u_{3,1}^{(m,n)} = 0, \quad (m, n) \in \mathbb{N}_3^2. \quad (4.34)$$

Define

$$\mathbf{u}_l^{(m,n)} = \left(u_{l,1}^{(m,n)}, u_{l,2}^{(m,n)}, \dots, u_{l,I}^{(m,n)}\right)^\top, \quad l = 1, 2, 3.$$

Using (4.34), we can rewrite the discrete system (4.18) with $l = 3$ in the matrix form

$$\left(\mathbf{A}_4^{(m,n)} + \mathbf{D}_1^{(m,n)}\right)\mathbf{u}_3^{(m,n)} + \mathbf{a}_I u_{3,I+1}^{(m,n)} = 0, \quad (m, n) \in \mathbb{N}_3^2, \quad (4.35)$$

where

$$\mathbf{A}_4^{(m,n)} = \begin{pmatrix} 1/\left(\left(1/r_{2,(JJ)}^{(m,n)} + 1\right)\frac{\varepsilon_1}{\varepsilon_2} + 1\right) - 2 & 1 & & & \\ & 1 & -2 & 1 & \\ & & \ddots & \ddots & \ddots \\ & & & 1 & -2 \end{pmatrix}, \quad \mathbf{a}_I = \begin{pmatrix} 0 \\ \vdots \\ 0 \\ 1 \end{pmatrix}.$$

and

$$\mathbf{D}_1^{(m,n)} = h^2 \left(\kappa_1^2 - \left(\frac{m\pi}{a}\right)^2 - \left(\frac{n\pi}{b}\right)^2 \right) \mathbf{I}_I.$$

Let

$$\mathbf{A}_4^{(m,n)} + \mathbf{D}_1^{(m,n)} = \mathbf{L}_4^{(m,n)} \mathbf{U}_4^{(m,n)}, \quad (m, n) \in \mathbb{N}_3^2 \quad (4.36)$$

be the LU-decomposition. It follows from (4.35)–(4.36) that

$$\mathbf{U}_4^{(m,n)} \mathbf{u}_3^{(m,n)} + \left(\mathbf{L}_4^{(m,n)}\right)^{-1} \mathbf{a}_I u_{3,I+1}^{(m,n)} = 0, \quad (m, n) \in \mathbb{N}_3^2, \quad (4.37)$$

where $\mathbf{U}_4^{(m,n)} = (r_{4,(pq)}^{(m,n)})$. It follows from (4.37) that

$$\mathbf{u}_3^{(m,n)} = -\left(\mathbf{U}_4^{(m,n)}\right)^{-1} \left(\mathbf{L}_4^{(m,n)}\right)^{-1} \mathbf{a}_I u_{3,I+1}^{(m,n)}, \quad (m, n) \in \mathbb{N}_3^2, \quad (4.38)$$

It is clear to note that the first equation of the system (4.38) is

$$u_{3,1}^{(m,n)} = (-1)^{2+I} \left(\det(\mathbf{U}_4^{(m,n)})\right)^{-1} u_{3,I+1}^{(m,n)}, \quad (m, n) \in \mathbb{N}_3^2. \quad (4.39)$$

Let

$$\mathbf{A}_3^{(m,n)} = \begin{pmatrix} 1/\left(1/r_{1,(JJ)}^{(m,n)} + 2\right) - 2 & 1 & & & \\ & -2 & 1 & & \\ & & \ddots & \ddots & \ddots \\ & & & 1 & -2 \end{pmatrix}_{I \times I}, \quad \mathbf{a}_1^{(m,n)} = \begin{pmatrix} -1 \\ 0 \\ \vdots \\ 0 \end{pmatrix}_{I \times 1},$$

where $(m, n) \in \mathbb{N}_1^2$ or $(m, n) \in \mathbb{N}_2^2$. Using (4.32), (4.34) and (4.39), we can write (4.18) with $l = 1$ in the following matrix form:

$$\left(\mathbf{A}_3^{(m,n)} + \mathbf{D}_1^{(m,n)}\right)\mathbf{u}_1^{(m,n)} + \mathbf{a}_I u_{1,I+1}^{(m,n)} = \mathbf{a}_1 d_1^{(m,n)} u_{3,I+1}^{(m,n)}, \quad (m, n) \in \mathbb{N}_1^2, \quad (4.40)$$

where

$$d_1^{(0,n)} = 0, \quad n = 1, 2, \dots, N,$$

and

$$d_1^{(m,n)} = \left(\frac{\left(\frac{\varepsilon_1}{\varepsilon_2} - 1\right)\frac{m\pi h}{a}}{1/r_{1,(JJ)}^{(m,n)} + 2}\right) \left(\frac{1}{\left(1/r_{2,(JJ)}^{(m,n)} + 1\right)\frac{\varepsilon_1}{\varepsilon_2} + 1}\right) \left(\frac{(-1)^{2+I}}{\det(\mathbf{U}_4^{(m,n)})}\right), \quad (m, n) \in \mathbb{N}_3^2.$$

Similarly, we can rewrite (4.18) with $l = 2$ in the following matrix form:

$$\left(\mathbf{A}_3^{(m,n)} + \mathbf{D}_1^{(m,n)}\right)\mathbf{u}_2^{(m,n)} + \mathbf{a}_I u_{2,I+1}^{(m,n)} = \mathbf{a}_1 d_2^{(m,n)} u_{3,I+1}^{(m,n)}, \quad (m, n) \in \mathbb{N}_2^2, \quad (4.41)$$

where

$$d_2^{(m,0)} = 0, \quad m = 1, 2, \dots, M,$$

and

$$d_2^{(m,n)} = \left(\frac{(\frac{\varepsilon_1}{\varepsilon_2} - 1) \frac{n\pi h}{b}}{1/r_{1,(JJ)}^{(m,n)} + 2} \right) \left(\frac{1}{(1/r_{2,(JJ)}^{(m,n)} + 1) \frac{\varepsilon_1}{\varepsilon_2} + 1} \right) \left(\frac{(-1)^{2+I}}{\det(\mathbf{U}_4^{(m,n)})} \right), \quad (m, n) \in \mathbb{N}_3^2.$$

Let

$$\mathbf{A}_3^{(m,n)} + \mathbf{D}_1^{(m,n)} = \mathbf{L}_3^{(m,n)} \mathbf{U}_3^{(m,n)}, \quad (m, n) \in \mathbb{N}_1^2 \text{ or } (m, n) \in \mathbb{N}_2^2, \quad (4.42)$$

be the LU-decomposition. It follows from (4.40)–(4.42) that

$$\mathbf{U}_3^{(m,n)} \mathbf{u}_l^{(m,n)} + (\mathbf{L}_3^{(m,n)})^{-1} \mathbf{a}_l \mathbf{u}_{l,I+1}^{(m,n)} = (\mathbf{L}_3^{(m,n)})^{-1} \mathbf{a}_l d_l^{(m,n)} \mathbf{u}_{3,I+1}^{(m,n)}, \quad (m, n) \in \mathbb{N}_l^2, l = 1, 2, \quad (4.43)$$

where $\mathbf{U}_3^{(m,n)} = (r_{3,(pq)}^{(m,n)})$.

Combining the last equations of the systems (4.43) and (4.37) gives

$$\begin{aligned} r_{3,(II)}^{(m,n)} u_{l,I} + u_{l,I+1} &= s_l^{(m,n)} \mathbf{u}_{3,I+1}^{(m,n)}, \quad (m, n) \in \mathbb{N}_l^2, \text{ for } l = 1, 2, \\ r_{4,(II)}^{(m,n)} u_{3,I} + u_{3,I+1} &= 0, \quad (m, n) \in \mathbb{N}_3^2, \end{aligned}$$

where $s_l^{(m,n)} = -\tilde{l}_{I1}^{(m,n)} d_l^{(m,n)}$, $l = 1, 2$, and $\tilde{l}_{I1}^{(m,n)}$ is the $(I, 1)$ -th entry of $(\mathbf{L}_3^{(m,n)})^{-1}$. We can write the above system in the matrix form

$$\begin{pmatrix} \mathbf{R}_4 & & \\ & \mathbf{R}_5 & \\ & & \mathbf{R}_6 \end{pmatrix} \begin{pmatrix} \mathbf{u}_{1,I} \\ \mathbf{u}_{2,I} \\ \mathbf{u}_{3,I} \end{pmatrix} + \begin{pmatrix} \hat{\mathbf{I}}_4 & -\mathcal{D}_1 \\ & \hat{\mathbf{I}}_5 & -\mathcal{D}_2 \\ & & \hat{\mathbf{I}}_6 \end{pmatrix} \begin{pmatrix} \mathbf{u}_{1,I+1} \\ \mathbf{u}_{2,I+1} \\ \mathbf{u}_{3,I+1} \end{pmatrix} = 0, \quad (4.44)$$

where

$$\begin{aligned} \mathbf{R}_4 &= \text{diag}(r_{3,(II)}^{(m,n)}), \quad (m, n) \in \mathbb{N}_1^2, \\ \mathbf{R}_5 &= \text{diag}(r_{3,(II)}^{(m,n)}), \quad (m, n) \in \mathbb{N}_2^2, \\ \mathbf{R}_6 &= \text{diag}(r_{4,(II)}^{(m,n)}), \quad (m, n) \in \mathbb{N}_3^2, \end{aligned}$$

the matrix \mathcal{D}_1 is the diagonal matrix $\text{diag}(s_1^{(m,n)})$, $(m, n) \in \mathbb{N}_1^2$ by deleting the column with respect to $m = 0$, and the matrix \mathcal{D}_2 is the diagonal matrix $\text{diag}(s_2^{(m,n)})$, $(m, n) \in \mathbb{N}_2^2$ by deleting the column with respect to $n = 0$.

Similar to the homogeneous medium case, the TBC (2.22) can be discretized as

$$\begin{pmatrix} \hat{\mathbf{I}}_1 & & \\ & \hat{\mathbf{I}}_2 & \\ & & \hat{\mathbf{I}}_3 \end{pmatrix} \begin{pmatrix} \mathbf{u}_{1,I} \\ \mathbf{u}_{2,I} \\ \mathbf{u}_{3,I} \end{pmatrix} + \begin{pmatrix} -\hat{\mathbf{I}}_1 - \mathbf{F}_1 - \mathbf{H}_1 & -\mathbf{G}_1 & \mathbf{I}_1 \\ & -\hat{\mathbf{I}}_2 - \mathbf{F}_2 - \mathbf{G}_2 & \mathbf{I}_2 \\ \mathbf{F}_3 & \mathbf{G}_3 & -\hat{\mathbf{I}}_3 \end{pmatrix} \begin{pmatrix} \mathbf{u}_{1,I+1} \\ \mathbf{u}_{2,I+1} \\ \mathbf{u}_{3,I+1} \end{pmatrix} = \begin{pmatrix} \mathbf{g}_1 \\ \mathbf{g}_2 \\ 0 \end{pmatrix}. \quad (4.45)$$

Using (4.44) and (4.45), we obtain

$$\begin{pmatrix} -\hat{\mathbf{I}}_1 - \mathbf{F}_1 - \mathbf{H}_1 - \mathbf{R}_4^{-1} & -\mathbf{G}_1 & \mathbf{I}_1 + \mathbf{R}_4^{-1} \mathcal{D}_1 \\ & -\hat{\mathbf{I}}_2 - \mathbf{F}_2 - \mathbf{G}_2 - \mathbf{R}_5^{-1} & \mathbf{I}_2 + \mathbf{R}_5^{-1} \mathcal{D}_2 \\ & \mathbf{F}_3 & -\hat{\mathbf{I}}_3 - \mathbf{R}_6^{-1} \end{pmatrix} \begin{pmatrix} \mathbf{u}_{1,I+1} \\ \mathbf{u}_{2,I+1} \\ \mathbf{u}_{3,I+1} \end{pmatrix} = \begin{pmatrix} \mathbf{g}_1 \\ \mathbf{g}_2 \\ 0 \end{pmatrix}. \quad (4.46)$$

The solution $\mathbf{E}_1 = (u_1, u_2, u_3)$ on the open aperture Γ can be obtained by solving the linear system (4.46).

Remark 4.1. For the cavity filled with a multi-layered medium (more than two layers), a similar discretization can be developed for each layer, and similar discrete continuity conditions can be deduced on the interface between every two neighboring layers. As a result, a linear system similar to (4.44) can be obtained for the electric field in the first layer below the ground plane. Consequently,

we can get a linear system on the open aperture of the cavity by using the linear system similar to (4.44)–(4.45). The solution \mathbf{E} on the open aperture Γ can be obtained by solving the resulting system.

5. EVALUATING SINGULAR INTEGRALS BASED ON THE FFT

One of the key issues in the algorithm is how to evaluate efficiently and accurately the singular integrals in (3.16)–(3.18). Due to the lack of closed form and the existence of singularity, direct numerical integration is notoriously expensive. In this section, we propose an efficient algorithm to evaluate these integrals based on the Fast Fourier Transform (FFT). Specifically, we consider the evaluation of integrals $\tilde{F}_{j,(k)}^{(m,n)}$, $\tilde{G}_{j,(k)}^{(m,n)}$, and $\tilde{H}_{j,(k)}^{(m,n)}$, $j = 1, 2$ for $(m, n) \in \mathbb{N}^2, k \in \mathbb{N}^2, \mathbb{N}^2 = \{0, 1, 2, \dots, M\} \times \{0, 1, 2, \dots, N\}$. We refer to Appendix A for the definition of $\tilde{F}_{2,(k)}^{(m,n)}$, $\tilde{G}_{2,(k)}^{(m,n)}$, and $\tilde{H}_{2,(k)}^{(m,n)}$.

5.1. Reduction of singularity. It is easy to see that $\tilde{F}_{j,(k)}^{(m,n)}$, $j = 1, 2$ are weakly singular integrals, while $\tilde{G}_{j,(k)}^{(m,n)}$, $\tilde{H}_{j,(k)}^{(m,n)}$, $j = 1, 2$ include Cauchy type singular integrals. To make the computation easier, we first apply the integration by parts to reduce the order of singularity

$$\begin{aligned} \tilde{G}_{1,(k)}^{(m,n)} &= \int_{\Gamma} \cos\left(\frac{m\pi x_1}{a}\right) \sin\left(\frac{n\pi x_2}{b}\right) \partial_{x_2} \left(\int_{\Gamma} \cos\left(\frac{k_1\pi y_1}{a}\right) \cos\left(\frac{k_2\pi y_2}{b}\right) g(\mathbf{x}, \mathbf{y}) ds_{\mathbf{y}} \right) ds_{\mathbf{x}} \\ &= \int_0^a \cos\left(\frac{m\pi x_1}{a}\right) \sin\left(\frac{n\pi x_2}{b}\right) \left(\int_{\Gamma} \cos\left(\frac{k_1\pi y_1}{a}\right) \cos\left(\frac{k_2\pi y_2}{b}\right) g(\mathbf{x}, \mathbf{y}) dy \right) \Big|_{x_2=0}^{x_2=b} dx_1 \\ &\quad - \int_{\Gamma} \partial_{x_2} \left(\cos\left(\frac{m\pi x_1}{a}\right) \sin\left(\frac{n\pi x_2}{b}\right) \right) \left(\int_{\Gamma} \cos\left(\frac{k_1\pi y_1}{a}\right) \cos\left(\frac{k_2\pi y_2}{b}\right) g(\mathbf{x}, \mathbf{y}) ds_{\mathbf{y}} \right) ds_{\mathbf{x}} \\ &= -\frac{n\pi}{b} \int_{\Gamma} \cos\left(\frac{m\pi x_1}{a}\right) \cos\left(\frac{n\pi x_2}{b}\right) \left(\int_{\Gamma} \cos\left(\frac{k_1\pi y_1}{a}\right) \cos\left(\frac{k_2\pi y_2}{b}\right) g(\mathbf{x}, \mathbf{y}) ds_{\mathbf{y}} \right) ds_{\mathbf{x}}. \end{aligned}$$

Similar simplifications can be done for the integrals $\tilde{G}_{2,(k)}^{(m,n)}$ and $\tilde{H}_{j,(k)}^{(m,n)}$, $j = 1, 2$. In the end, we only need to consider evaluating the following three integrals:

$$\begin{aligned} I_{1,(k)}^{(m,n)} &= \int_{\Gamma} \cos\left(\frac{m\pi x_1}{a}\right) \sin\left(\frac{n\pi x_2}{b}\right) \left(\int_{\Gamma} \cos\left(\frac{k_1\pi y_1}{a}\right) \sin\left(\frac{k_2\pi y_2}{b}\right) g(\mathbf{x}, \mathbf{y}) ds_{\mathbf{y}} \right) ds_{\mathbf{x}}, \\ I_{2,(k)}^{(m,n)} &= \int_{\Gamma} \sin\left(\frac{m\pi x_1}{a}\right) \cos\left(\frac{n\pi x_2}{b}\right) \left(\int_{\Gamma} \sin\left(\frac{k_1\pi y_1}{a}\right) \cos\left(\frac{k_2\pi y_2}{b}\right) g(\mathbf{x}, \mathbf{y}) ds_{\mathbf{y}} \right) ds_{\mathbf{x}}, \\ I_{3,(k)}^{(m,n)} &= \int_{\Gamma} \cos\left(\frac{m\pi x_1}{a}\right) \cos\left(\frac{n\pi x_2}{b}\right) \left(\int_{\Gamma} \cos\left(\frac{k_1\pi y_1}{a}\right) \cos\left(\frac{k_2\pi y_2}{b}\right) g(\mathbf{x}, \mathbf{y}) ds_{\mathbf{y}} \right) ds_{\mathbf{x}}. \end{aligned}$$

They belong to the same type of integrals, i.e.,

$$I_{(k)}^{(m,n)} = \int_{\Gamma} \exp\left(\frac{m\pi x_1}{a}i\right) \exp\left(\frac{n\pi x_2}{b}i\right) \left(\int_{\Gamma} \exp\left(\frac{k_1\pi y_1}{a}i\right) \exp\left(\frac{k_2\pi y_2}{b}i\right) g(\mathbf{x}, \mathbf{y}) ds_{\mathbf{y}} \right) ds_{\mathbf{x}}.$$

Next, we propose a fast algorithm to evaluate $I_{(k)}^{(m,n)}$ by using the FFT.

5.2. Algorithm for $I_{(k)}^{(m,n)}$ based on the FFT. Without loss of generality, we may assume $a \geq b$. To evaluate the integral $I_{(k)}^{(m,n)}$, we first consider evaluating the inner integral

$$I_k(x_1, x_2) = \int_{\Gamma} \exp\left(\frac{k_1\pi y_1}{a}i\right) \exp\left(\frac{k_2\pi y_2}{b}i\right) g(\mathbf{x}, \mathbf{y}) dy$$

for fixed $k_1, k_2 \in \mathbb{N}$ and $\mathbf{x} \in \Gamma$.

Define two functions:

$$f_{\text{Rect}}(x_1, x_2) = \begin{cases} 1, & \text{if } (x_1, x_2) \in \Gamma, \\ 0, & \text{otherwise,} \end{cases}$$

and

$$f_{\text{Circ}}(r) = \begin{cases} 1, & \text{if } r \leq \sqrt{2}a, \\ 0, & \text{otherwise.} \end{cases}$$

Then

$$I_k(x_1, x_2) = \int_{\mathbb{R}^2} \exp\left(\frac{k_1\pi y_1}{a}i\right) \exp\left(\frac{k_2\pi y_2}{b}i\right) f_{\text{Rect}}(y_1, y_2) g(\mathbf{x}, \mathbf{y}) f_{\text{Circ}}(|\mathbf{x} - \mathbf{y}|) d\mathbf{y}, \quad \mathbf{x} \in \Gamma.$$

Define

$$F(\mathbf{y}) = \exp\left(\frac{k_1\pi y_1}{a}i\right) \exp\left(\frac{k_2\pi y_2}{b}i\right) f_{\text{Rect}}(y_1, y_2)$$

and

$$G(\mathbf{x} - \mathbf{y}) = g(\mathbf{x}, \mathbf{y}) f_{\text{Circ}}(|\mathbf{x} - \mathbf{y}|).$$

Then

$$I_k(x_1, x_2) = \int_{\mathbb{R}^2} F(\mathbf{y}) G(\mathbf{x} - \mathbf{y}) ds_{\mathbf{y}},$$

which is a convolution and can be efficiently evaluated by using the FFT. Denote by $\mathcal{F}(\cdot)$ the Fourier transform and $\mathcal{F}^{-1}(\cdot)$ the inverse Fourier transform. Clearly, we have from the Fourier transformation that

$$I_k(x_1, x_2) = \mathcal{F}^{-1}(\mathcal{F}(F) \cdot \mathcal{F}(G)).$$

For $(j_1, j_2) \in \mathbb{N}^2$, it is easy to see that

$$\begin{aligned} \mathcal{F}(F)(j_1, j_2) &= \int_{\mathbb{R}^2} e^{-2\pi i(j_1 y_1 + j_2 y_2)} F(\mathbf{y}) d\mathbf{y} \\ &= \int_{\Gamma} e^{-2\pi i(j_1 y_1 + j_2 y_2)} \exp\left(\frac{k_1\pi y_1}{a}i\right) \exp\left(\frac{k_2\pi y_2}{b}i\right) d\mathbf{y} \\ &= \frac{(e^{-2\pi j_1 a + k_1\pi} - 1)}{(-2\pi j_1 + k_1\pi/a)i} \frac{(e^{-2\pi j_2 b + k_2\pi} - 1)}{(-2\pi j_2 + k_2\pi/b)i}. \end{aligned}$$

Denote by B the disk centered at the origin with radius $\sqrt{2}a$. The following integral formula is convenient to evaluate $\mathcal{F}(G)(j_1, j_2)$:

$$\begin{aligned} \mathcal{F}(G)(j_1, j_2) &= \int_{\mathbb{R}^2} e^{-2\pi i(j_1 y_1 + j_2 y_2)} G(\mathbf{y}) ds_{\mathbf{y}} \\ &= \int_B e^{-2\pi i(j_1 y_1 + j_2 y_2)} g(\mathbf{0}, \mathbf{y}) ds_{\mathbf{y}} \\ &= \frac{1}{4\pi} \int_0^{\sqrt{2}a} \int_0^{2\pi} e^{-2\pi i(j_1 r \cos \theta + j_2 r \sin \theta)} \frac{e^{i\kappa_0 r}}{r} r d\theta dr \\ &= \frac{1}{4\pi} \int_0^{\sqrt{2}a} J_0\left(2\pi \sqrt{j_1^2 + j_2^2} r\right) e^{i\kappa_0 r} dr, \end{aligned}$$

where $J_0(\cdot)$ is the Bessel function of order zero.

Let $R = \sqrt{2}a$ and $c = 2\pi \sqrt{j_1^2 + j_2^2}$. Since there is no closed form for the integral

$$I = \int_0^R J_0(cr) e^{i\kappa_0 r} dr$$

with $R > 0$ and $c > 0$, we need an algorithm to evaluate I numerically.

We may assume R and the wavenumber κ_0 are both $\mathcal{O}(1)$. Since $c = 2\pi\sqrt{j_1^2 + j_2^2}$ can be very large for $(j_1, j_2) \in \mathbb{N}^2$, in order to evaluate I accurately, we consider two cases:

- (1) Case 1: j_1 and j_2 are small, say, $\max\{|j_1|, |j_2|\} \leq 10$, so that c is $\mathcal{O}(1)$. In this case, direct integration by using a high order Gaussian quadrature would efficiently evaluate the integral I .
- (2) Case 2: j_1 and j_2 are large, in which case c is large and $J_0(cr)$ is highly oscillatory. We can make use of the asymptotic formula

$$J_0(z) = \sqrt{\frac{2}{\pi z}} \left(\cos(z - \pi/4) + \frac{\sin(z - \pi/4)}{8z} + \mathcal{O}\left(\frac{1}{z^2}\right) \right),$$

which is quite accurate for $z \gg 1$ if we drop the reminder. Another useful formula is

$$\int_0^\infty J_0(cr) e^{i\kappa_0 r} dr = \frac{1}{c^2 - \kappa_0^2}, \text{ for } c > \kappa_0.$$

Therefore,

$$\begin{aligned} I &= \frac{1}{c^2 - \kappa_0^2} - \int_R^\infty J_0(cr) e^{i\kappa_0 r} dr \\ &= \frac{1}{c^2 - \kappa_0^2} - \frac{1}{c} \int_{cR}^\infty J_0(z) e^{i\kappa_0 z/c} dz \\ &\approx \frac{1}{c^2 - \kappa_0^2} - \frac{1}{c} \sqrt{\frac{2}{\pi}} \int_{cR}^\infty \left(\frac{\cos(z - \pi/4)}{\sqrt{z}} + \frac{\sin(z - \pi/4)}{8z^{3/2}} \right) e^{i\kappa_0 z/c} dz \\ &= \frac{1}{c^2 - \kappa_0^2} - \frac{1}{c} \sqrt{\frac{2}{\pi}} \int_{cR}^\infty \left(\frac{e^{(z-\pi/4)i} + e^{(\pi/4-z)i}}{2\sqrt{z}} + \frac{e^{(z-\pi/4)i} - e^{(z-\pi/4)i}}{2i8z^{3/2}} \right) e^{i\kappa_0 z/c} dz. \end{aligned}$$

In other words, we have to evaluate these two kinds of integrals

$$\int_{R_0}^\infty \frac{e^{pzi}}{\sqrt{z}} dz, \quad \int_{R_0}^\infty \frac{e^{qzi}}{z^{3/2}} dz,$$

where $p, q \in \mathbb{R}$ and $R_0 \gg 1$. They belong to the same type of integrals. In fact, we obtain from the integration by parts that

$$\int_{R_0}^\infty \frac{e^{qzi}}{z^{3/2}} dz = 2 \frac{e^{qR_0 i}}{\sqrt{R_0}} + 2qi \int_{R_0}^\infty \frac{e^{qzi}}{\sqrt{z}} dz.$$

On the other hand,

$$\int_{R_0}^\infty \frac{e^{pzi}}{\sqrt{z}} dz = \frac{\sqrt{\pi}}{2p} \left(1 + i - 2\text{Fresnelc}(\sqrt{2pR_0/\pi}) - 2i\text{Fresnels}(\sqrt{2pR_0/\pi}) \right),$$

where $\text{Fresnelc}(\cdot)$ and $\text{Fresnels}(\cdot)$ are Fresnel cosine and sine integrals, respectively. To efficiently evaluate them, we make use of the following asymptotic expansions for $z \gg 1$:

$$\begin{aligned} \text{Fresnelc}(z) &= \frac{1}{2} + f(z) \sin\left(\frac{1}{2}\pi z^2\right) - g(z) \cos\left(\frac{1}{2}\pi z^2\right), \\ \text{Fresnels}(z) &= \frac{1}{2} - f(z) \cos\left(\frac{1}{2}\pi z^2\right) - g(z) \sin\left(\frac{1}{2}\pi z^2\right), \end{aligned}$$

where

$$\begin{aligned} f(z) &= \frac{1}{\pi z} \left(1 - \frac{3}{(\pi z^2)^2} + \mathcal{O}\left(\frac{1}{z^8}\right) \right), \\ g(z) &= \frac{1}{\pi^2 z^3} \left(1 - \frac{15}{(\pi z^2)^2} + \mathcal{O}\left(\frac{1}{z^8}\right) \right). \end{aligned}$$

Combining all the ingredients above, we are able to efficiently evaluate the inner integral $I_k(x_1, x_2)$. Once $I_k(x_1, x_2)$ is available, for the outer integral with respect to \boldsymbol{x} , we simply use the trapezoidal rule, in which case the FFT can also be directly applied.

6. IMPLEMENTATION AND COMPLEXITY

Our algorithm is extremely efficient in terms of computational cost. A detailed analysis on the computational complexity of Algorithm I for the electromagnetic scattering by an open rectangular cavity filled with a homogeneous medium and Algorithm II for the electromagnetic scattering by an open rectangular cavity filled with a layered medium.

Algorithm I: Electromagnetic scattering by a homogeneous cavity.

- Step 1 Generate the matrices $\boldsymbol{F}_i, \boldsymbol{G}_i, \boldsymbol{H}_i, i = 1, 2$ and the vectors $\boldsymbol{g}_i, i = 1, 2$;
 Step 2 Calculate the LU decomposition to get $\boldsymbol{U}_i^{(m,n)}, i = 1, 2$ and $\boldsymbol{R}_i^{-1}, i = 1, 2, 3$ by using the forward Gaussian elimination with a row partial pivoting;
 Step 3 Solve the system (3.35) for $\boldsymbol{E}_{i,J+1}, i = 1, 2, 3$.
-

Algorithm II: Electromagnetic scattering by a layered cavity.

- Step 1 Generate the matrices $\boldsymbol{F}_i, \boldsymbol{G}_i, \boldsymbol{H}_i, i = 1, 2$ and the vectors $\boldsymbol{g}_i, i = 1, 2$;
 Step 2 Calculate the LU decomposition to get $\boldsymbol{U}_i^{(m,n)}, i = 1, 2$ and $\boldsymbol{R}_i^{-1}, i = 1, 2, 3$ by using the forward Gaussian elimination with a row partial pivoting. Further, calculate the LU decomposition to get $\boldsymbol{U}_i^{(m,n)}, \boldsymbol{U}_i^{(m,n)}, i = 3, 4$ $\boldsymbol{D}_i, i = 1, 2$ and $\boldsymbol{R}_i^{-1}, i = 4, 5, 6$;
 Step 3 Solve the system (4.46) for \boldsymbol{E} on the open aperture Γ .
-

The cost for each step is presented in Table 1. In Step 1, one needs to calculate the singular integrals to generate the matrices $\boldsymbol{F}_i, \boldsymbol{G}_i, \boldsymbol{H}_i, i = 1, 2$. As shown in Section 5, we evaluate the singular integrals based on FFT, which requires only $MN(MN \log(MN) + MN \log(MN))$ complex operations for all the singular integrals. Hence the overall cost of Step 1 is $O(M^2N^2 \log(MN))$. In Step 2 for Algorithm I, we need to calculate the LU decomposition for $\boldsymbol{A}_1 + \boldsymbol{D}^{(m,n)}, (m, n) \in \mathbb{N}_1^2 \cup \mathbb{N}_2^2$ and $\boldsymbol{A}_2 + \boldsymbol{D}^{(m,n)}, (m, n) \in \mathbb{N}_3^2$. By noting the tridiagonal structure of these matrices, only $3J(M+1)(N+1) + 3JMN$ complex operations are needed. In Step 2 for Algorithm II, the cost for calculating the LU decomposition in the bottom layer is $3J(M+1)(N+1) + 3JMN$, and the cost for calculating the LU decomposition in the top layer is $5I(M+1)(N+1) + 3IMN$. In Algorithms I and II, we need to solve the interface system (3.35) and (4.46), respectively. We point out that a direct method, such as the Gaussian elimination scheme, requires $(3MN + 2N)^3/3$ complex operations, which is not efficient. In order to solve the interface system effectively, we may need the effective iterative solver. The efficiency of the iterative algorithm for the interface system depends upon many factors, such as the complicated transparent boundary condition, the regularity of solution, the eigenvalue distribution and the condition numbers of the coefficient matrix. We will carry out the related work in the follow-up work.

7. NUMERICAL EXPERIMENTS

In this section, several numerical examples are presented to demonstrate the the performance of the proposed method. Throughout all the examples, the incident wave

$$\boldsymbol{E}^{\text{inc}}(\boldsymbol{x}) = (\cos \alpha \hat{\boldsymbol{\theta}} + \sin \alpha \hat{\boldsymbol{\phi}}) e^{i\kappa_0 d r},$$

TABLE 1. The computational complexity of Algorithms I and II.

| Step | Homogeneous cavity | Layered cavity |
|------|-----------------------|---|
| 1 | $O(M^2 N^2 \log(MN))$ | $O(M^2 N^2 \log(MN))$ |
| 2 | $3J((M+1)(N+1) + MN)$ | $3J(M+1)(N+1) + 3JMN$ $+5I(M+1)(N+1) + 3IMN$ |
| 3 | $(3MN + 2N)^3/3$ | $(3MN + 2N)^3/3$ |

where α is the polarization angle, $\hat{\theta}$ and $\hat{\phi}$ are the standard unit vectors in the spherical coordinates, and \mathbf{d} is the incident direction given by

$$\mathbf{d} = -(\sin \theta \cos \phi, \sin \theta \sin \phi, \cos \theta).$$

The wavenumber $\kappa_0 = 2\pi$. The incident angle $\phi = 0$ so that we focus on the xz -plane.

The physical quantity of interest associated with the cavity scattering is the radar cross section (RCS), which measures the detectability of a target by a radar system [12]. When the incident angle and the observation angle are the same, the RCS is called the backscatter RCS. The specific formulas can be found in [10] for the RCS of the three-dimensional cavity-backed apertures.

Our fast algorithm is mainly validated and compared with the adaptive finite element PML method. The fast algorithm is carried out by a laptop with Intel(R) Core(TM) i5-2430M CPU @ 2.40GHz. The implementation of the adaptive finite element PML method is based on parallel hierarchical grid (PHG) [18, 25], which is a toolbox for developing parallel adaptive finite element programs on unstructured tetrahedral meshes. The linear system resulted from the finite element discretization is solved by MUMPS (MUltifrontal Massively Parallel Sparse direct Solver) [17], which is a general purpose library for the direct solution of large linear systems. The computation is done on the high performance computers of State Key Laboratory of Scientific and Engineering Computing, Chinese Academy of Sciences, in which each node has 2 Intel Xeon Gold 6140 CPUs (2.3 GHz, 18 cores) and 192 GB memory and a 100 GB EDR Infiniband network is used for data communication between nodes. We solve the finite element problem for each θ with one node (36 cores). The maximum number of degrees of freedom (DoFs) on the mesh are between 2,000,000 and 3,000,000. The running time (CPU time/cores) is 5 to 10 minutes. By choosing the increment of θ as $\Delta\theta = 0.5^\circ$, the finite element problem is solved 100 times in Example 1, and 180 times in Examples 2 and 3.

When presenting the numerical results, we use the following notations:

- M, N : Number of modes for the Fourier expansions in the x_1 and x_2 directions, respectively.
- J : Number of partition points along the x_3 direction. For a two-layered medium, another variable I is used.
- T_{singular} : Amount of time in seconds required to evaluate the singular integrals.
- T_{assemble} : Amount of time in seconds required to assemble the matrix.
- T_{solve} : Amount of time in seconds required to solve the linear system.
- T_{RCS} : Amount of time in seconds required to calculate the RCS.

7.1. Example 1. In this example, we consider the cavity filled with a homogeneous medium. First, the backscatter RCS of the cavity with size $a = b = 10\lambda$ and $c = 30\lambda$ is calculated. The RCS of $\hat{\theta}\hat{\theta}$ and $\hat{\phi}\hat{\phi}$ polarizations are shown in Figure 3 for various incident angle θ . The numerical results show excellent agreement with the calculations by the mode matching method presented in [3] and the modal approach presented in [15]. The detailed computational time is given in Table 2. Most of the time is spent on the evaluation of singular integrals. However, we only need to compute them once for different incident angles. In addition, most of the applications only require a small number of modes to resolve the field. Next, the backscatter radar cross section of a cavity with size $a = b = \lambda$ and $c = 3\lambda$ is calculated by the fast algorithm and the adaptive finite element PLM method. Figure 4 shows the RCS versus θ for $\hat{\theta}\hat{\theta}$ and $\hat{\phi}\hat{\phi}$ polarizations. The backscatter RCS is shown as red solid lines and blue circles for the fast algorithm and adaptive PML method, respectively. It is clear to note

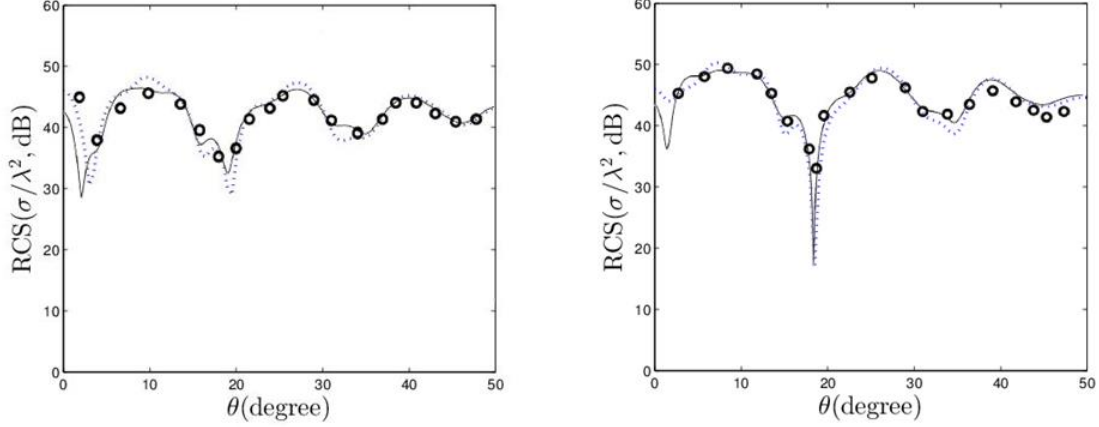


FIGURE 3. Example 1: the backscatter RCS of the cavity with size $a = b = 10\lambda$ and $c = 30\lambda$. The dashed line is the RCS calculated by our fast algorithm, the solid line is the RCS calculated by the mode matching method presented in [3], and the circle is the RCS calculated by the modal approach presented in [15].

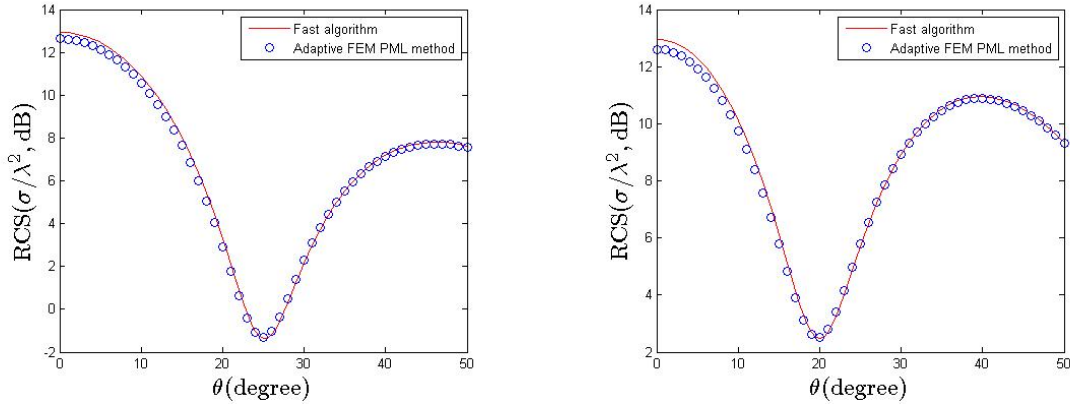


FIGURE 4. Example 1: the backscatter RCS of the cavity with size $a = b = \lambda$ and $c = 3\lambda$.

that the results obtained by both methods are consistent with each other. Detailed computational time is given in Table 3.

TABLE 2. Example 1: The time of the computation for the cavity size $a = b = \lambda, c = 3\lambda$ with $\alpha = 0, \theta = \pi/6$.

| M, N | J | T_{singular} | T_{assemble} | T_{solve} | T_{RCS} |
|--------------|------|-----------------------|-----------------------|--------------------|------------------|
| $M = N = 21$ | 1000 | 119.697858 | 0.307505 | 0.286226 | 0.006255 |
| $M = N = 3$ | 1000 | 4.100736 | 0.002453 | 0.000072 | 0.000715 |
| $M = N = 3$ | 600 | 4.013451 | 0.002015 | 0.000066 | 0.000691 |

7.2. Example 2. In this example, we consider the cavity filled with a material having a relative permittivity $\epsilon_r = 7 + 1.5i$ and a constant magnetic permeability $\mu = 1$. The backscatter RCS of the cavity with size $a = \lambda$, and $b = c = 0.25\lambda$ is calculated. The RCS of $\hat{\theta}\hat{\theta}$ and $\hat{\phi}\hat{\phi}$ polarizations are shown in Figure 5 for various incident angle θ . The results based on the fast algorithm and the

TABLE 3. Example 1: The time of the computation for the cavity size $a = b = 10\lambda, c = 30\lambda$ with $\alpha = 0, \theta = \pi/6$.

| M, N | J | T_{singular} | T_{assemble} | T_{solve} | T_{RCS} |
|--------------|------|-----------------------|-----------------------|--------------------|------------------|
| $M = N = 21$ | 1000 | 212.170604 | 0.298627 | 0.335862 | 0.006811 |
| $M = N = 15$ | 1000 | 155.201708 | 0.062623 | 0.058558 | 0.003075 |
| $M = N = 15$ | 1500 | 155.360674 | 0.063114 | 0.038757 | 0.006100 |

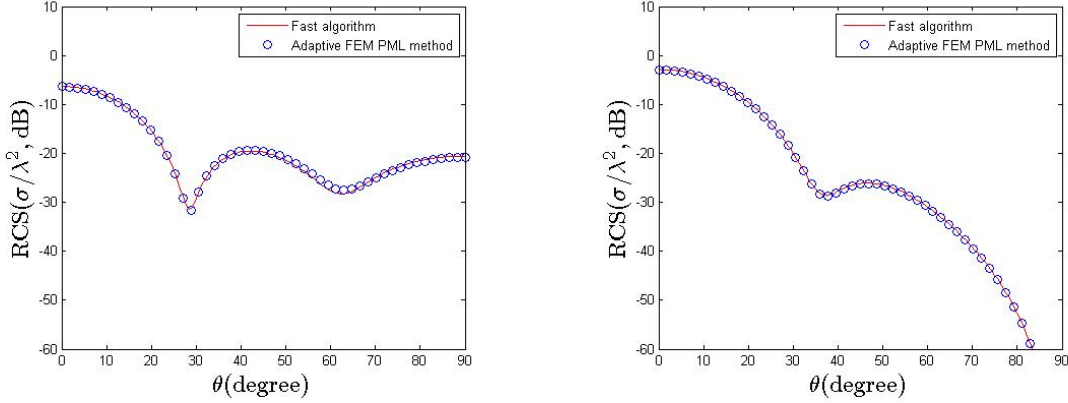


FIGURE 5. Example 2: the backscatter RCS of the cavity with size $a = \lambda$ and $b = c = 0.25\lambda$.

adaptive PML method are again in excellent agreement. Detailed computational time is given in Table 4. Again, the cost is dominated by the evaluation of singular integrals.

TABLE 4. Example 2: The time of the computation for the cavity size $a = \lambda, b = c = 0.25\lambda$ with $\alpha = 0, \theta = \pi/2$.

| M, N | J | T_{singular} | T_{assemble} | T_{solve} | T_{RCS} |
|--------------|------|-----------------------|-----------------------|--------------------|------------------|
| $M = N = 15$ | 1000 | 43.997846 | 0.065300 | 0.051353 | 0.003815 |
| $M = N = 3$ | 1000 | 3.037277 | 0.001508 | 0.000068 | 0.001106 |
| $M = N = 3$ | 100 | 3.047187 | 0.001897 | 0.000098 | 0.001130 |

7.3. Example 3. This example is concerned with the cavity filled with a two-layer material. The cavity size is $a = b = \lambda$ and $c = 3\lambda$. The top and bottom layer materials have parameters $\epsilon_r = 7 + 1.5i$ and $\epsilon_r = 3 + 0.05i$, respectively. The thickness of the top material and the bottom material are $c_1 = \lambda$ and $c_2 = 2\lambda$, respectively. The backscatter RCS of $\hat{\theta}\hat{\theta}$ and $\hat{\phi}\hat{\phi}$ polarizations are shown in Figure 6 for various incident angle θ . Once again, both methods are consistent with each other very well. Detailed computational time is given in Table 5. It can be seen that the total computational time is less than three minutes by using our fast algorithm.

TABLE 5. Example 3: The time of the computation for the cavity size $a = b = \lambda, c_1 = \lambda, c_2 = 2\lambda$ with $\alpha = 0, \theta = \pi/2$.

| M, N | J, I | T_{singular} | T_{assemble} | T_{solve} | T_{RCS} |
|--------------|----------------------|-----------------------|-----------------------|--------------------|------------------|
| $M = N = 21$ | $J = 1000, I = 2000$ | 130.499710 | 0.329729 | 0.341623 | 0.006732 |
| $M = N = 3$ | $J = 1000, I = 2000$ | 4.075719 | 0.002566 | 0.000097 | 0.001600 |
| $M = N = 3$ | $J = 100, I = 200$ | 4.194746 | 0.002448 | 0.000075 | 0.001176 |

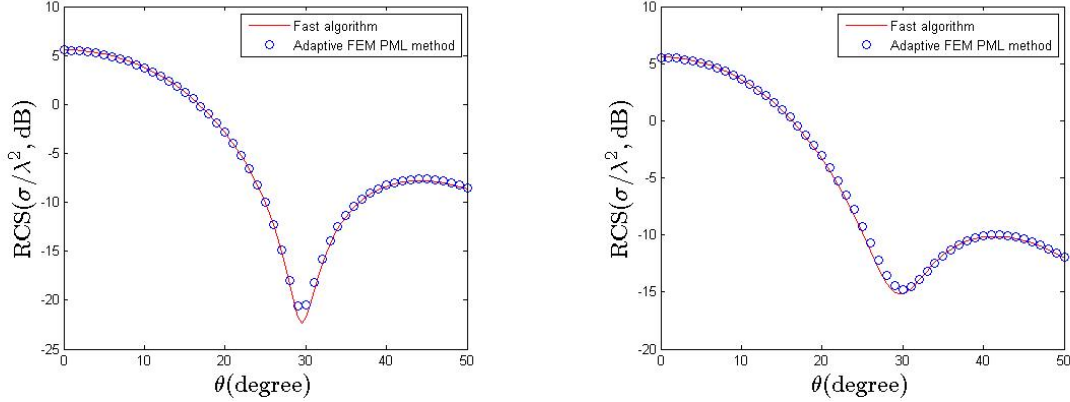


FIGURE 6. Example 3: The backscatter RCS of the cavity with size $a = b = \lambda$, $c_1 = \lambda$ and $c_2 = 2\lambda$.

8. CONCLUSION

In this paper, we have presented a fast algorithm for the electromagnetic scattering from three dimensional open rectangular cavities. Based on the Fourier series expansions in the horizontal directions and the Gaussian elimination along the vertical direction, the fast algorithm reduces the global system to an interface system on the open aperture only. We also propose an efficient algorithm to evaluate the singular integrals on the aperture based on FFT. The whole algorithm enjoys the advantage of the low computational cost by solving only the coefficients of the modes of the Fourier series. Moreover, our fast algorithm has the capability of handling large cavities or high wave numbers. This work provides a viable alternative to the current efforts of designing sophisticated basis functions for solving Maxwell equations with high wave numbers or large cavities. A possible future work is to extend our fast algorithm to the optimal design problems and inverse problems. It is of particular interest in designing the shape and composition of a layered cavity to minimize the RCS [4, 5]. Computationally, the design problem can be challenging because of the need of solving the scattering problem repeatedly. The fast algorithm presented here certainly would provide an efficient and accurate numerical tool for these problems.

APPENDIX A. NOTATIONS

In the appendix, we list the expressions of the entries for the vectors used in (3.20).

The definitions of \mathbf{F}_1 , \mathbf{G}_1 and \mathbf{H}_1 are given by

$$\mathbf{F}_1 := \begin{pmatrix} \mathbf{F}_1^{(0)} \\ \mathbf{F}_1^{(1)} \\ \vdots \\ \mathbf{F}_1^{(M)} \end{pmatrix}, \quad \mathbf{G}_1 := \begin{pmatrix} \mathbf{G}_1^{(0)} \\ \mathbf{G}_1^{(1)} \\ \vdots \\ \mathbf{G}_1^{(M)} \end{pmatrix}, \quad \mathbf{H}_1 := \begin{pmatrix} \mathbf{H}_1^{(0)} \\ \mathbf{H}_1^{(1)} \\ \vdots \\ \mathbf{H}_1^{(M)} \end{pmatrix},$$

with

$$\mathbf{F}_1^{(m)} := \begin{pmatrix} \mathbf{F}_1^{(m,1)} \\ \mathbf{F}_1^{(m,2)} \\ \vdots \\ \mathbf{F}_1^{(m,N)} \end{pmatrix}, \quad \mathbf{G}_1^{(m)} := \begin{pmatrix} \mathbf{G}_1^{(m,1)} \\ \mathbf{G}_1^{(m,2)} \\ \vdots \\ \mathbf{G}_1^{(m,N)} \end{pmatrix}, \quad \mathbf{H}_1^{(m)} := \begin{pmatrix} \mathbf{H}_1^{(m,1)} \\ \mathbf{H}_1^{(m,2)} \\ \vdots \\ \mathbf{H}_1^{(m,N)} \end{pmatrix},$$

where

$$\begin{aligned} \mathbf{F}_1^{(m,n)} &:= \left(\mathbf{F}_{1,(0)}^{(m,n)} \quad \mathbf{F}_{1,(1)}^{(m,n)} \quad \cdots \quad \mathbf{F}_{1,(M)}^{(m,n)} \right), & \mathbf{F}_{1,(k_1)}^{(m,n)} &:= \left(F_{1,(k_1,1)}^{(m,n)} \quad F_{1,(k_1,2)}^{(m,n)} \quad \cdots \quad F_{1,(k_1,N)}^{(m,n)} \right), \\ \mathbf{G}_1^{(m,n)} &:= \left(\mathbf{G}_{1,(1)}^{(m,n)} \quad \mathbf{G}_{1,(2)}^{(m,n)} \quad \cdots \quad \mathbf{G}_{1,(M)}^{(m,n)} \right), & \mathbf{G}_{1,(k_1)}^{(m,n)} &:= \left(G_{1,(k_1,0)}^{(m,n)} \quad G_{1,(k_1,1)}^{(m,n)} \quad \cdots \quad G_{1,(k_1,N)}^{(m,n)} \right), \\ \mathbf{H}_1^{(m,n)} &:= \left(\mathbf{H}_{1,(0)}^{(m,n)} \quad \mathbf{H}_{1,(1)}^{(m,n)} \quad \cdots \quad \mathbf{H}_{1,(M)}^{(m,n)} \right), & \mathbf{H}_{1,(k_1)}^{(m,n)} &:= \left(H_{1,(k_1,1)}^{(m,n)} \quad H_{1,(k_1,2)}^{(m,n)} \quad \cdots \quad H_{1,(k_1,N)}^{(m,n)} \right). \end{aligned}$$

The definitions of \mathbf{g}_1 and $\mathbf{E}_{l,j}$ with $l = 1, 2, 3$, $0 \leq j \leq J + 1$ are given by

$$\begin{aligned} \mathbf{g}_1 &:= \left(\mathbf{g}_1^{(0)} \quad \mathbf{g}_1^{(1)} \quad \cdots \quad \mathbf{g}_1^{(M)} \right)^\top, & \mathbf{g}_1^{(m)} &:= \left(g_1^{(m,1)} \quad g_1^{(m,2)} \quad \cdots \quad g_1^{(m,N)} \right), \\ \mathbf{E}_{1,j} &:= \left(\mathbf{E}_{1,j}^{(0)} \quad \mathbf{E}_{1,j}^{(1)} \quad \cdots \quad \mathbf{E}_{1,j}^{(M)} \right)^\top, & \mathbf{E}_{1,j}^{(m)} &:= \left(E_{1,j}^{(m,1)} \quad E_{1,j}^{(m,2)} \quad \cdots \quad E_{1,j}^{(m,N)} \right), \\ \mathbf{E}_{2,j} &:= \left(\mathbf{E}_{2,j}^{(1)} \quad \mathbf{E}_{2,j}^{(2)} \quad \cdots \quad \mathbf{E}_{2,j}^{(M)} \right)^\top, & \mathbf{E}_{2,j}^{(m)} &:= \left(E_{2,j}^{(m,0)} \quad E_{2,j}^{(m,1)} \quad \cdots \quad E_{2,j}^{(m,N)} \right), \\ \mathbf{E}_{3,j} &:= \left(\mathbf{E}_{3,j}^{(1)} \quad \mathbf{E}_{3,j}^{(2)} \quad \cdots \quad \mathbf{E}_{3,j}^{(M)} \right)^\top, & \mathbf{E}_{3,j}^{(m)} &:= \left(E_{3,j}^{(m,1)} \quad E_{3,j}^{(m,2)} \quad \cdots \quad E_{3,j}^{(m,N)} \right). \end{aligned}$$

The definitions of \mathbf{F}_2 , \mathbf{G}_2 and \mathbf{H}_2 are given by

$$\mathbf{F}_2 := \begin{pmatrix} \mathbf{F}_2^{(1)} \\ \mathbf{F}_2^{(2)} \\ \vdots \\ \mathbf{F}_2^{(M)} \end{pmatrix}, \quad \mathbf{G}_2 := \begin{pmatrix} \mathbf{G}_2^{(1)} \\ \mathbf{G}_2^{(2)} \\ \vdots \\ \mathbf{G}_2^{(M)} \end{pmatrix}, \quad \mathbf{H}_2 := \begin{pmatrix} \mathbf{H}_2^{(1)} \\ \mathbf{H}_2^{(2)} \\ \vdots \\ \mathbf{H}_2^{(M)} \end{pmatrix},$$

with

$$\mathbf{F}_2^{(m)} := \begin{pmatrix} \mathbf{F}_2^{(m,0)} \\ \mathbf{F}_2^{(m,1)} \\ \vdots \\ \mathbf{F}_2^{(m,N)} \end{pmatrix}, \quad \mathbf{G}_2^{(m)} := \begin{pmatrix} \mathbf{G}_2^{(m,0)} \\ \mathbf{G}_2^{(m,1)} \\ \vdots \\ \mathbf{G}_2^{(m,N)} \end{pmatrix}, \quad \mathbf{H}_2^{(m)} := \begin{pmatrix} \mathbf{H}_2^{(m,0)} \\ \mathbf{H}_2^{(m,1)} \\ \vdots \\ \mathbf{H}_2^{(m,N)} \end{pmatrix},$$

where

$$\begin{aligned} \mathbf{F}_2^{(m,n)} &:= \left(\mathbf{F}_{2,(1)}^{(m,n)} \quad \mathbf{F}_{2,(2)}^{(m,n)} \quad \cdots \quad \mathbf{F}_{2,(M)}^{(m,n)} \right), & \mathbf{F}_{2,(k_1)}^{(m,n)} &:= \left(F_{2,(k_1,0)}^{(m,n)} \quad F_{2,(k_1,1)}^{(m,n)} \quad \cdots \quad F_{2,(k_1,N)}^{(m,n)} \right), \\ \mathbf{G}_2^{(m,n)} &:= \left(\mathbf{G}_{2,(1)}^{(m,n)} \quad \mathbf{G}_{2,(2)}^{(m,n)} \quad \cdots \quad \mathbf{G}_{2,(M)}^{(m,n)} \right), & \mathbf{G}_{2,(k_1)}^{(m,n)} &:= \left(G_{2,(k_1,0)}^{(m,n)} \quad G_{2,(k_1,1)}^{(m,n)} \quad \cdots \quad G_{2,(k_1,N)}^{(m,n)} \right), \\ \mathbf{H}_2^{(m,n)} &:= \left(\mathbf{H}_{2,(0)}^{(m,n)} \quad \mathbf{H}_{2,(1)}^{(m,n)} \quad \cdots \quad \mathbf{H}_{2,(M)}^{(m,n)} \right), & \mathbf{H}_{2,(k_1)}^{(m,n)} &:= \left(H_{2,(k_1,1)}^{(m,n)} \quad H_{2,(k_1,2)}^{(m,n)} \quad \cdots \quad H_{2,(k_1,N)}^{(m,n)} \right), \end{aligned}$$

and

$$F_{2,(k)}^{(m,n)} := \frac{h}{c^{(m,n)}} 2\kappa_0^2 \tilde{F}_{2,(k)}^{(m,n)}, \quad G_{2,(k)}^{(m,n)} := \frac{h}{c^{(m,n)}} \frac{2k_1\pi}{a} \tilde{G}_{2,(k)}^{(m,n)}, \quad H_{2,(k)}^{(m,n)} := \frac{h}{c^{(m,n)}} \frac{-2k_2\pi}{b} \tilde{H}_{2,(k)}^{(m,n)},$$

with

$$\begin{aligned} \tilde{F}_{2,(k)}^{(m,n)} &:= \int_{\Gamma} \sin\left(\frac{m\pi x_1}{a}\right) \cos\left(\frac{n\pi x_2}{b}\right) \left(\int_{\Gamma} \sin\left(\frac{k_1\pi y_1}{a}\right) \cos\left(\frac{k_2\pi y_2}{b}\right) g(\mathbf{x}, \mathbf{y}) d\mathbf{s}_{\mathbf{y}} \right) d\mathbf{s}_{\mathbf{x}}, \\ \tilde{G}_{2,(k)}^{(m,n)} &:= \int_{\Gamma} \sin\left(\frac{m\pi x_1}{a}\right) \cos\left(\frac{n\pi x_2}{b}\right) \left(\int_{\Gamma} \cos\left(\frac{k_1\pi y_1}{a}\right) \cos\left(\frac{k_2\pi y_2}{b}\right) \partial_{x_1} g(\mathbf{x}, \mathbf{y}) d\mathbf{s}_{\mathbf{y}} \right) d\mathbf{s}_{\mathbf{x}}, \\ \tilde{H}_{2,(k)}^{(m,n)} &:= \int_{\Gamma} \sin\left(\frac{m\pi x_1}{a}\right) \cos\left(\frac{n\pi x_2}{b}\right) \left(\int_{\Gamma} \cos\left(\frac{k_1\pi y_1}{a}\right) \cos\left(\frac{k_2\pi y_2}{b}\right) \partial_{x_1} g(\mathbf{x}, \mathbf{y}) d\mathbf{s}_{\mathbf{y}} \right) d\mathbf{s}_{\mathbf{x}}. \end{aligned}$$

Here

$$c^{(m,n)} = \begin{cases} \frac{ab}{2}, & \text{if } n = 0, \\ \frac{ab}{4}, & \text{others.} \end{cases}$$

The definition of \mathbf{g}_2 is given by

$$\mathbf{g}_2 := \left(\mathbf{g}_2^{(1)} \quad \mathbf{g}_2^{(2)} \quad \dots \quad \mathbf{g}_2^{(M)} \right), \quad \mathbf{g}_2^{(m)} := \left(g_1^{(m,0)} \quad g_1^{(m,1)} \quad \dots \quad g_1^{(m,N)} \right),$$

where

$$g_2^{(m,n)} := \frac{h}{c^{(m,n)}} 2(i\alpha_2 p_3 + i\beta p_2) \int_{\Gamma} \sin\left(\frac{m\pi x_1}{a}\right) \cos\left(\frac{n\pi x_2}{b}\right) e^{i(\alpha_1 x_1 + \alpha_2 x_2)} d\mathbf{s}_{\mathbf{x}}.$$

REFERENCES

- [1] A. Aziz, R. Kellogg, and A. Stephen, A two point boundary value problem with a rapidly oscillating solution, *Numer. Math.*, 53 (1988), 107–121.
- [2] I. Babuska and S. Sauter, Is the pollution effect of the FEM avoidable for the Helmholtz equation considering high wave number?, *SIAM J. Numer. Anal.*, 34 (1997), 2392–2423.
- [3] G. Bao, J. Gao, J. Lin, and W. Zhang, Mode matching for the electromagnetic scattering from three-dimensional large cavities, *IEEE Trans. Antennas Propagat.*, 60 (2012), 2004–2010.
- [4] G. Bao and J. Lai, Radar cross section reduction of a cavity in the ground plane, *Commun. Comput. Phys.*, 15 (2014), 895–910.
- [5] G. Bao and J. Lai, Optimal shape design of a cavity for radar cross section reduction, *SIAM J. Control Optim.*, 52 (2014), 2122–2140.
- [6] G. Bao and W. Sun, A fast algorithm for the electromagnetic scattering from a large cavity, *SIAM J. Sci. Comput.*, 27 (2005), 553–574.
- [7] K. Du, A composite preconditioner for the electromagnetic scattering from a large cavity, *J. Comput. Phys.*, 230 (2011), 8089–8108.
- [8] K. Du, W. Sun, and X. Zhang, Arbitrary high-order C^0 tensor product Galerkin finite element methods for the electromagnetic scattering from a large cavity, *J. Comput. Phys.*, 242 (2013) 181–195.
- [9] S. Hawkins, K. Chen, and P. Harris, On the influence of the wavenumber on compression in a wavelet boundary element method for the Helmholtz equation, *Int. J. Numer. Anal. Mod.*, 4 (2007), 48–62.
- [10] J. Jin, A finite element-boundary integral formulation for scattering by three-dimensional cavity-backed apertures, *IEEE Trans. Antennas Propagat.*, 39 (1991), 97–104.
- [11] J. Jin and J. L. Volakis, A hybrid finite element method for scattering and radiation by micro strip patch antennas and arrays residing in a cavity, *IEEE Trans. Antennas Propagat.*, 39 (1991), 1598–1604.
- [12] J. Jin, *The Finite Element Method in Electromagnetics*, Wiley & Son, New York, 2002.
- [13] J. Lai, S. Ambikasaran, and L. Greengard, A fast direct solve for high frequency scattering from a large cavity in two dimensions, *SIAM J. Sci. Comput.*, 36 (2014), B887–B903.
- [14] J. Lai and L. Greengard, and M. O’Neil, Robust integral formulations for electromagnetic scattering from three-dimensional cavities, *J. Comput. Phys.*, 345 (2017), 1–16.
- [15] H. Ling, S. Lee, and R. Chou, High-frequency RCS of the open cavities with rectangular and circular cross sections, *IEEE Trans. Antennas Propagat.*, 37 (1989), 648–654.
- [16] H. Li, H. Ma, and W. Sun, Legendre spectral Galerkin method for electromagnetic scattering from large cavities, *SIAM J. Numer. Anal.*, 51 (2013), 253–276.
- [17] Mumps: a multifrontal massively parallel sparse direct solver, <http://mumps.enseeiht.fr/>.
- [18] PHG (Parallel Hierarchical Grid), <http://lsec.cc.ac.cn/phg/>.
- [19] T. Van and A. Wood, Finite element analysis for 2-D cavity problem, *IEEE Trans. Antennas Propag.*, 51 (2003), 1–8.
- [20] Y. Wang, K. Du, and W. Sun, A second-order method for the electromagnetic scattering from a large cavity, *Numer. Math. Theor. Meth. Appl.*, 1 (2008), 357–382.
- [21] C. Wang and Y. Gan, 2D cavity modeling using method of moments and iterative solvers, *Progress In Electromagnetics Research*, PiEr, 43 (2003), 123–142.
- [22] W. Wood and A. Wood, Development and numerical solution of integral equations for electromagnetic scattering from a trough in a ground plane, *IEEE Trans. Antennas Propag.*, 47 (1999), 1318–1322.
- [23] X. Yuan, G. Bao, and P. Li, An adaptive finite element DtN method for the open cavity scattering problems, *CSIAM Trans. Appl. Math.*, to appear.
- [24] D. Zhang, F. Ma, and H. Dong, A finite element method with rectangular perfectly matched layers for the scattering from cavities, *J. Comput. Math.*, 27 (2009), 812–834.
- [25] L. Zhang, W. Zheng, B. Lu, T. Cui, W. Leng, and D. Lin, The toolbox PHG and its applications, *SCIENTIA SINICA Informationis*, 46 (2016), 1442–1464.
- [26] M. Zhao, Z. Qiao, and T. Tang, A fast high order method for electromagnetic scattering by large open cavities, *J. Comput. Math.*, 29 (2011), 278–304.

- [27] M. Zhao and N. Zhu, A fast precondition iterative method for the electromagnetic scattering by multiple cavities with high wave numbers, *J. Comput. Phys.*, 398 (2019), 108826.

DEPARTMENT OF MATHEMATICS, NORTHEASTERN UNIVERSITY, SHENYANG 110819, CHINA
E-mail address: chenyanli@mail.neu.edu.cn

SCHOOL OF MATHEMATICS, FACULTY OF SCIENCE, BEIJING UNIVERSITY OF TECHNOLOGY, BEIJING, 100124, CHINA.

E-mail address: jxue@lsec.cc.ac.cn

SCHOOL OF MATHEMATICAL SCIENCES, ZHEJIANG UNIVERSITY HANGZHOU, ZHEJIANG 310027, CHINA
E-mail address: laijun6@zju.edu.cn

DEPARTMENT OF MATHEMATICS, PURDUE UNIVERSITY, WEST LAFAYETTE, INDIANA 47907, USA
E-mail address: lipeijun@math.purdue.edu